Nontraumatic Pediatric Head and Neck Emergencies: Resource for On-Call Radiologists

Alexandra M. Foust, DO • Lindsey Johnstone, MD • Rekha Krishnasarma, MD • Dann C. Martin, MD • Jennifer Vaughn, MD
Karuna Shekdar, MD • Elizabeth Snyder, MD • Ty Todd, DO • Sumit Pruthi, MBBS • Asha Sarma, MD

Author affiliations, funding, and conflicts of interest are listed at the end of this article.

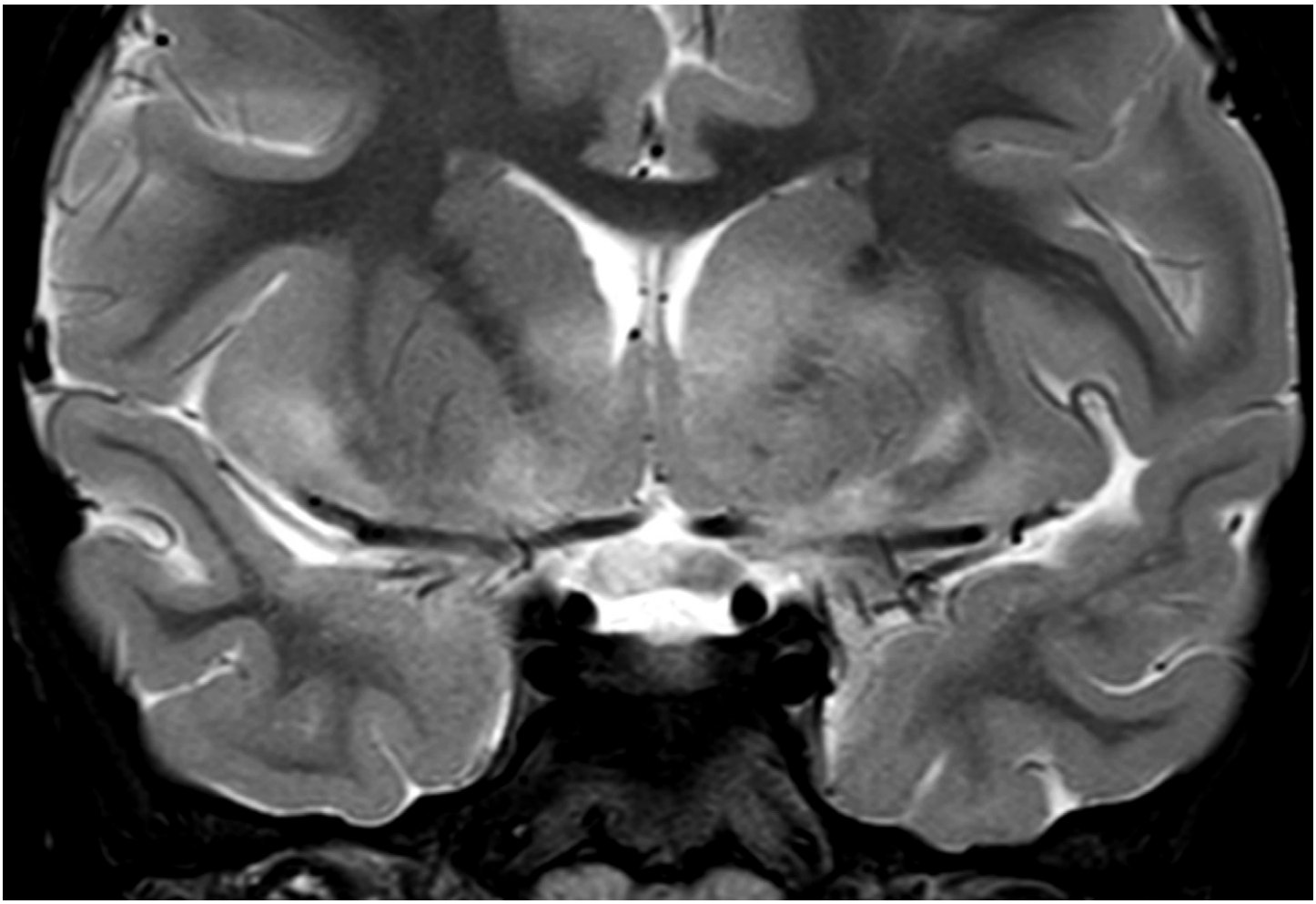

The vast array of acute nontraumatic diseases encountered in the head and neck of pediatric patients can be intimidating for radiologists in training in a fast-paced emergency setting. Although there is some overlap of pediatric and adult diseases, congenital lesions and developmental variants are much more common in the pediatric population. Furthermore, the relative incidences of numerous infections and neoplasms differ between pediatric and adult populations. Young patients and/or those with developmental delays may have clinical histories that are difficult to elicit or nonspecific presentations, underscoring the importance of imaging in facilitating accurate and timely diagnoses. It is essential that radiologists caring for children be well versed in pediatric nontraumatic head and neck emergency imaging. The authors provide an on-call resource for radiology trainees, organized by anatomic location and highlighting key points, pearls, pitfalls, and mimics of many acute nontraumatic diseases in the pediatric head and neck.

©RSNA, 2024 • *radiographics.rsna.org*

RG

ENHANCING IMAGING INTERPRETATION
IN SPECIAL SETTINGS

This copy is for personal use only. To order copies, contact *reprints@rsna.org*

Supplemental Material | TestYour Knowledge | CME

RadioGraphics 2024; 44(10):e240027
https://doi.org/10.1148/rg.240027

Content Codes: CT, ER, MR, NR

Abbreviations: CECT = contrast-enhanced CT, FS = fat suppressed, ON = optic nerve, T1W = T1 weighted, T2W = T2 weighted

TEACHING POINTS

- Regardless of the underlying cause of proptosis, a stretched appearance of the optic nerve (ON) and tenting of the posterior globe (ie, "guitar pick" sign) are critical imaging findings of orbital compartment syndrome. This emergent vision-threatening condition due to increased intraorbital pressure may result in ON ischemia.
- Imaging of juvenile nasopharyngeal angiofibroma (JNA) reveals a well-marginated soft-tissue mass centered at the sphenopalatine foramen.
- Although similar in size to a coin, a button battery has a distinctive "double-ring" appearance on frontal radiographs and a "beveled-edge" appearance on lateral radiographs.
- Suppurative retropharyngeal lymphadenitis can be complicated by rupture of the nodal abscess into the retropharyngeal space. At CECT, the resultant retropharyngeal abscess has convex borders and peripheral enhancement ("football" shaped) in contradistinction to reactive retropharyngeal effusion, which has a bow tie shape and no peripheral enhancement.
- Coalescence is diagnosed when erosion of the mastoid septa and/or bony cortex occurs and distinguishes coalescent mastoiditis from simple mastoid effusion or "incipient mastoiditis," which is commonly seen with otitis media or even in asymptomatic patients.

Introduction

Acute head and neck diseases, infections in particular, are a frequent reason for pediatric emergency department visits (1,2). Given differences in the anatomy and relative incidence of various diseases between children and adults, radiology trainees must be familiar with pediatric-specific considerations to guide optimal and timely management.

In this article, a location-based approach is used to review imaging of acute nontraumatic head and neck diseases in pediatric patients. The complementarity of multiple imaging modalities is summarized, and key clinical and radiologic findings of infectious, inflammatory, and vascular diseases are reviewed. In addition, pediatric-specific normal variants and differential considerations are discussed.

Imaging Modalities

Table 1 provides a summary of the most common indications, technique considerations, and relative advantages of radiography, US, CT, and MRI for emergent evaluation of pediatric head and neck diseases. Modality selection is based on multiple factors including *(a)* which modality will depict the suspected disease process most comprehensively, *(b)* availability, *(c)* capability to minimize lengthy acquisitions and associated procedural sedation, *(d)* capability to comply with the ALARA principle (limiting the patient's ionizing radiation exposure to a level as low as reasonably achievable), and *(e)* cost (3,4). US and contrast-enhanced CT (CECT) are the most commonly used first-line modalities. Pediatric-specific CT protocols can be used to minimize ionizing radiation exposure (5).

Disease Processes Categorized by Anatomic Region

Orbital Disease

Preseptal and Postseptal Cellulitis.—Orbital infections are a common indication for imaging in the pediatric emergency setting. Radiologists are often enlisted to differentiate between preseptal (periorbital) cellulitis and more severe postseptal (orbital) cellulitis, which have different treatment considerations. The Chandler classification system is used to assign orbital infectious diseases into five groups: group I, preseptal cellulitis; group II, orbital cellulitis without abscess; group III, subperiosteal abscess; group IV, orbital abscess; and group V, cavernous sinus thrombosis (6). Preseptal cellulitis is typically managed with oral antibiotics on an outpatient basis, while postseptal cellulitis necessitates intravenous antibiotic therapy and potentially surgical drainage of larger subperiosteal abscesses (7,8).

Affected pediatric patients present with painful, erythematous, and swollen-appearing periorbital soft tissues. Symptoms of orbital cellulitis tend to be more severe and include fever, restricted ocular movement, vision impairment, and proptosis. The most common cause of preseptal cellulitis is local trauma (eg, insect bite or skin infection), while postseptal cellulitis is most often a complication of sinusitis.

The orbital septum, a fibrous connective tissue sheet extending from the orbital periosteum to the tarsal plates of the eyelids, separating the periorbital and intraorbital fat, is the key anatomic landmark separating the preseptal and postseptal tissues. Medially, the orbital septum separates from the medial palpebral ligament, attaching to the posterior crest of the lacrimal bone (9). Laterally, it extends to attach to the orbital margin approximately 1.5 mm anterior to the lateral palpebral ligament orbital tubercle attachment. Practically speaking, the septum is not well seen on images, and its location can be inferred by drawing a line between the anterior-most aspect of the lateral and medial orbital rims to the tarsal plate on axial images (Fig 1) (9).

In preseptal cellulitis, CECT shows inflammatory changes of fat stranding and swelling superficial to the orbital septum. Contrarily, in postseptal cellulitis, intraorbital inflammation deep to the orbital septum may be extraconal (outside the extraocular muscle cone) and/or intraconal (inside the extraocular muscular cone). Subperiosteal abscesses are the most common complication and occur most frequently along the medial or superior orbit due to adjacent ethmoid or frontal sinus disease. These abscesses are often best seen in the coronal or sagittal plane as lenticular rim-enhancing fluid collections closely apposed to the orbit wall (Fig 1) (6).

It is important to note that the thinner pediatric skull and valveless emissary facial veins may provide a route for intracranial spread (7). Potential complications overlap with those of complicated sinusitis, but with a higher predilection for cavernous sinus thrombosis due to superior ophthalmic vein thrombophlebitis (Fig S1). Differential considerations include intraorbital vascular anomalies, neoplasms, and idiopathic orbital inflammatory syndrome (IOIS).

Table 1: Most Common Indications, Technique Considerations, and Relative Advantages of Radiography, US, CT, and MRI for Evaluating Pediatric Patients with Nontraumatic Emergent Head and Neck Conditions

Modality	Common Indications	Technique Considerations	Advantages	Disadvantages
Radiography	Acute stridor or upper airway obstruction (eg, croup, epiglottitis) Suspected airway or upper gastrointestinal tract foreign body Selected cases of pharyngitis	Anteroposterior and lateral views	Lower ionizing radiation dose compared with CT Useful for gross assessment of airway narrowing and radiopaque foreign bodies No procedural sedation needed	Less sensitive and specific for numerous conditions (thus, limited uses) compared with cross-sectional modalities May not show radiolucent foreign bodies
US	Palpable superficial abnormalities: mass, abscess, complicated cyst, selected vascular abnormalities, lymphadenitis	Including color with or without spectral Doppler High-frequency transducer is a "workhorse"	Portable, high availability Insensitivity to motion: short acquisition precludes need for sedation Lack of ionizing radiation exposure Low cost High image contrast resolution: excellent for differentiating cysts from solid masses Excellent assessment of vessels and lesion vascularity	Operator dependent Poor visualization of deep structures, inability to penetrate gas or bone
CT	Workhorse modality, used for imaging a broad range of infections and masses	Pediatric-specific protocols decrease radiation dose Intravenous iodinated contrast material generally indicated Split intravenous contrast agent bolus technique (half bolus, wait 3 minutes, administer second half of bolus) may be helpful for simultaneous evaluation of vessels and soft tissue Dual-energy or spectral CT may be helpful in cases of hemorrhage or calcifications Optional CT venography may be useful in some instances	Rapid (usually avoids sedation) Widely available High spatial resolution with excellent lesion localization, including in deep neck spaces Excellent bone detail, especially useful in infections involving the craniofacial bones or cervical spine	Tissue contrast resolution for lesion characterization may be inferior to that with US and MRI
MRI	Optic neuritis Complicated head and neck infections (including brain imaging) Complementary to CT for complicated sinogenic, otogenic, or angioinvasive fungal infections Osteomyelitis (complementary to CT) Soft-tissue masses or congenital lesions (often follow-up nonemergent evaluation)	Performed without and with intravenous contrast material for most indications Key sequences include fluid-sensitive (eg, T2W FS or STIR), noncontrast T1W (marrow, fat), DWI (for infections, congenital lesions; non-EPI preferred), and postcontrast T1W FS sequences Optional MR angiography, MR venography, 3D MPRAGE/FSPGR/BRAVO, arterial spin labeling (noncontrast perfusion) may be useful for some conditions	Excellent soft-tissue contrast resolution for lesion characterization Sensitive to bone marrow edema in craniofacial bones and cervical spine Useful for detection of intracranial or spinal complications of infection	Often less available than CT or US Longer examination time (greater need for sedation; motion artifact is problematic in children) Gadolinium deposition in tissues Poor visualization at airbone interfaces

Note.—BRAVO = three-dimensional (3D) T1-weighted (T1W) brain volume (GE HealthCare sequence), DWI = diffusion-weighted imaging, EPI = echo-planar imaging, FS = fat suppressed, FSPGR = fast spoiled gradient echo, MPRAGE = magnetization-prepared rapid gradient echo, STIR = short-tau inversion recovery, T2W = T2 weighted.

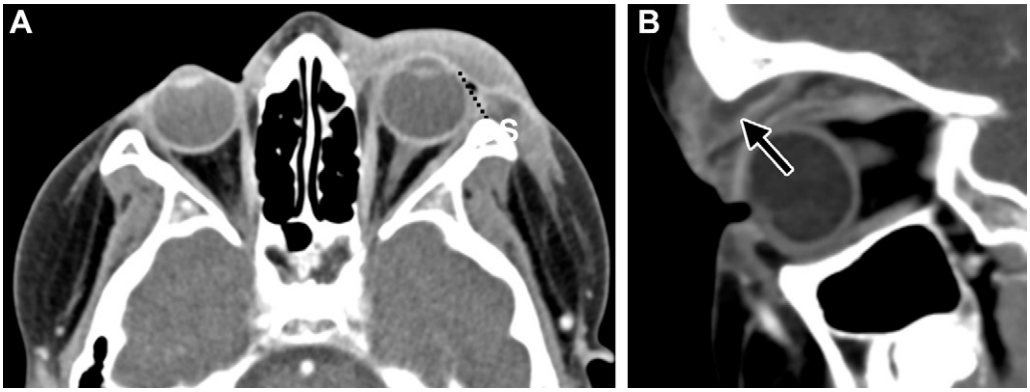

Figure 1. Orbital cellulitis in a 7-year-old patient with eye pain and swelling. **(A)** Axial CECT image shows marked preseptal soft-tissue swelling with subtle fat stranding deep to the orbital septum *(OS)* (dotted line). **(B)** Sagittal CECT image shows a lenticular peripherally enhancing subperiosteal abscess (arrow) extending along the orbital roof with surrounding postseptal extraconal fat stranding.

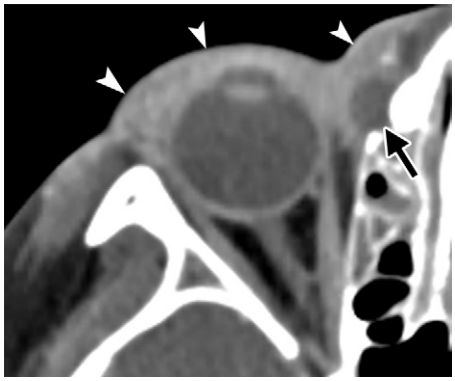

Figure 2. Dacryocystitis in a pediatric patient with medial eye swelling. Axial CECT image shows a rim-enhancing fluid collection (arrow) at the medial canthus, with adjacent preseptal cellulitis (arrowheads). A medial canthal location is key in differentiating dacryocystitis from sinogenic subperiosteal abscesses, which tend to occur more posteriorly along the superomedial orbit in postseptal cellulitis.

Dacryocystitis.—Dacryocystitis is lacrimal sac inflammation resulting from nasolacrimal duct (NLD) obstruction and subsequent infection. Congenital NLD obstruction results from failed perforation of the valve of Hasner. The incidence of NLD obstruction is high, occurring in up to 20% of neonates, and up to 96% of cases resolve spontaneously in the first year of life (10). Although dacryocystitis is most common in infants, a second narrowing more cephalic at the valve of Rosenmuller can act as a one-way valve, leading to mucocele formation (dacryocystocele). NLD mucoceles are associated with a higher infection risk than NLD obstruction alone (11).

Imaging reveals an enlarged nasolacrimal sac, which extends from the medial canthus to the inferior meatus (opening below the inferior nasal turbinate) with surrounding fat stranding (Fig 2). Dacryocystitis can incite preseptal cellulitis. The differential diagnosis includes dermoid or epidermoid cyst and naso-orbital cephalocele. Treatment consists of systemic antibiotics and in some cases, NLD probing.

Orbital Compartment Syndrome.—Acute proptosis (Fig 3) is best assessed in the axial plane at the level of the lenses. Distances measured from a perpendicular line between the two zygomatic processes to the anterior globe surfaces exceeding 21 mm indicate proptosis (12). Acute proptosis frequently results from retro-ocular (retrobulbar) space-occupying lesions in a normal-sized bony orbit. This is distinct from "exorbitism," in which the orbital contents chronically protrude from congenitally small bony orbits (eg, in craniosynostosis or craniofacial syndromes).

Regardless of the underlying cause of proptosis, a stretched appearance of the optic nerve (ON) and tenting of the posterior globe (ie, "guitar pick" sign) are critical imaging findings of orbital compartment syndrome. This emergent vision-threatening condition due to increased intraorbital pressure may result in ON ischemia (13).

It is important for radiologists on call to recognize the imaging finding of proptosis (defined as anterior protrusion of the globe from the bony orbit), which can be caused by numerous underlying conditions in pediatric patients. The differential diagnosis includes orbital cellulitis, vascular anomalies, rapidly growing neoplasms (eg, infantile hemangioma), idiopathic orbital inflammatory syndrome, trauma, and carotid cavernous fistula (Table 2) (12,14).

Papilledema Related to Elevated Intracranial Pressure.—Identifying the imaging finding of papilledema (elevated ON head) in the pediatric emergency setting is important, as it leads the radiologist to look for many potential underlying causes of the increased intracranial pressure. Brain imaging plays a key role in identifying the underlying cause, with possibilities including hydrocephalus, hemorrhage, neoplasm, infection, cerebral edema, venous thrombosis, and idiopathic intracranial hypertension (Fig 4). Clinical signs of elevated intracranial pressure such as new headache and early-morning emesis raise concern. Papilledema is generally first diagnosed at fundoscopic examination.

MRI findings of papilledema include flattened posterior globe, elevated optic papilla, and tortuous distended ON sheath complex (Fig 4) (15). There may be prelaminar ON enhancement, although the purpose of contrast material administration is generally evaluation of causal intracranial disease. Pseudopapilledema, or optic disc elevation at ophthalmologic examination related to structural factors such as optic disc drusen, is an alternative diagnosis that may be suggested if punctate calcifications are seen on CT images (16).

Table 2: Differential Diagnosis Considerations for Pediatric Proptosis

Disease	Patient Age	Helpful Features	Key Imaging Features
Neoplastic			
Hemangioma	Infant (highly unlikely after infancy)	Other infantile hemangiomas, red or blue skin discoloration	Avid arterial enhancement Internal flow voids
Rhabdomyosarcoma	Any age; majority younger than 10 y	Painless, with or without eyelid edema, chemosis	Restricted diffusion Heterogeneous solid mass
Lymphoma	Older children	Painless proptosis	Restricted diffusion More homogeneous solid mass
Optic glioma	Majority ≤10 y	Neurofibromatosis type 1	Fusiform masslike enlargement of ON; mass effect and/or proptosis is unusual
Neuroblastoma metastasis	<5 y	…	Lytic osseous lesion with secondary extension into orbit, predilection for greater sphenoid wing
Langerhans cell histiocytosis	Any age; peak age <5 y	"Beveled edge" osseous lesions are helpful	Lytic osseous lesion with secondary extension into orbit, soft-tissue mass
Nonneoplastic			
Idiopathic orbital inflammatory syndrome	Any age	No adjacent sinus disease, painful	Unilateral or bilateral orbital inflammation Extraocular muscle myotendinous junction enhancement
Slow-flow vascular anomaly (LM or VM)*	Any age; mainly in early childhood	Acute presentation with hemorrhage and/or infection (LM) or thrombosis (VM)	Phleboliths (VM) Fluid-fluid levels (LM)
Carotid-cavernous fistula	Any age	History of acute or subacute prior trauma, connective tissue disorder	Dilated superior ophthalmic vein and ipsilateral cavernous sinus

Sources.—References 12 and 13.
* LM = lymphatic malformation, VM = venous malformation.

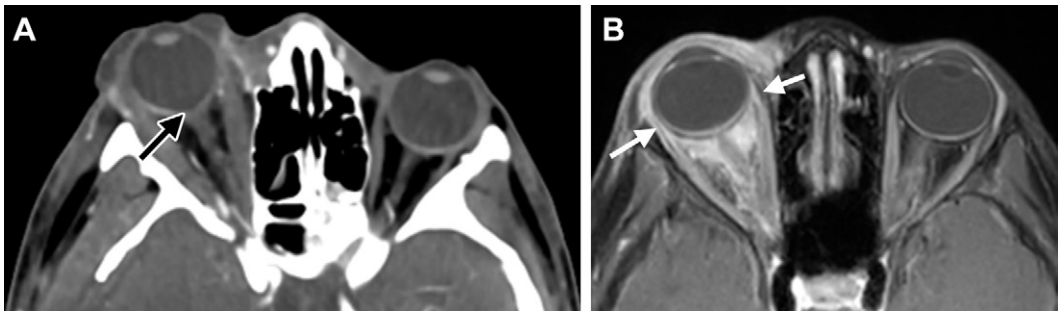

Figure 3. Proptosis in two pediatric patients. **(A)** Axial CECT image in a 14-year-old adolescent boy with central skull base fractures shows marked proptosis, stretching of the optic nerve (ON), and tenting (ie, "guitar pick" sign) (arrow) of the posterior globe. **(B)** Axial contrast-enhanced fat-suppressed (FS) T1-weighted (T1W) MR image in a 7-year-old girl with idiopathic orbital inflammatory syndrome shows right proptosis, bilateral intraorbital inflammatory change (greater on the right than on the left), and enhancing extraocular muscles (including the myotendinous junctions [arrows]).

Optic Neuritis.—Inflammatory (most common), infectious, or metabolic disorders may cause optic neuritis, or inflammation of the ON. Affected patients may present with acute or subacute vision loss. Interestingly, pediatric patients are more likely than adult patients to present with signs of bilateral optic neuritis and less likely to report pain with eye movement (17).

Contrast-enhanced MRI of the orbits is used to detect disease and to define the laterality and longitudinal extent of ON involvement. Craniospinal MRI is often indicated for identification of associated demyelinating central nerve system lesions in disorders such as multiple sclerosis, neuromyelitis optica, and myelin oligodendrocyte glycoprotein antibody–associated disease.

MRI reveals ON enlargement with T2 prolongation and enhancement (Fig 5). There may be associated ON sheath enhancement and perineural inflammation. The location and length of ON involvement may narrow the differential diagnosis (Table 3, Fig S2) (17,18). The differential diagnosis for optic neuritis includes optic glioma and ischemic optic neuropathy. Clinical history and other neuroimaging findings can aid in determining the diagnosis.

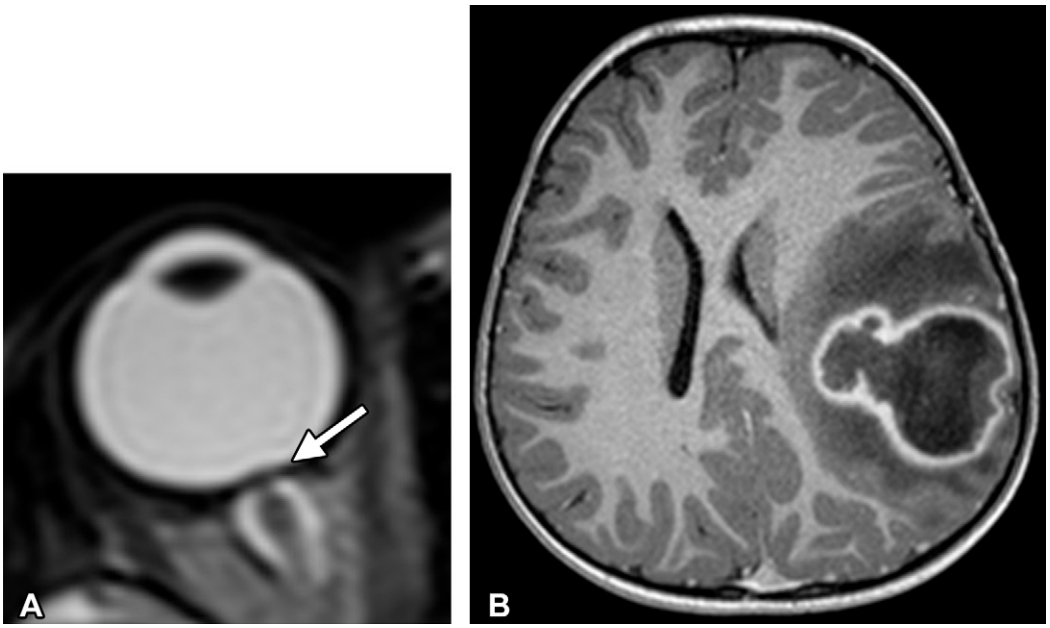

Figure 4. Papilledema secondary to a large cerebral abscess and associated elevated intracranial pressure in a 3-year-old patient. **(A)** Axial T2-weighted (T2W) FS MR image shows flattening of the posterior globe with subtle elevation of the ON head (arrow) and distention (>7.5 mm) of the ON sheath. **(B)** Axial contrast-enhanced T1W MR image of the brain shows a large peripherally enhancing abscess in the left frontoparietal region, with surrounding T1-hypointense vasogenic edema. The abscess showed corresponding marked restricted diffusion (not shown).

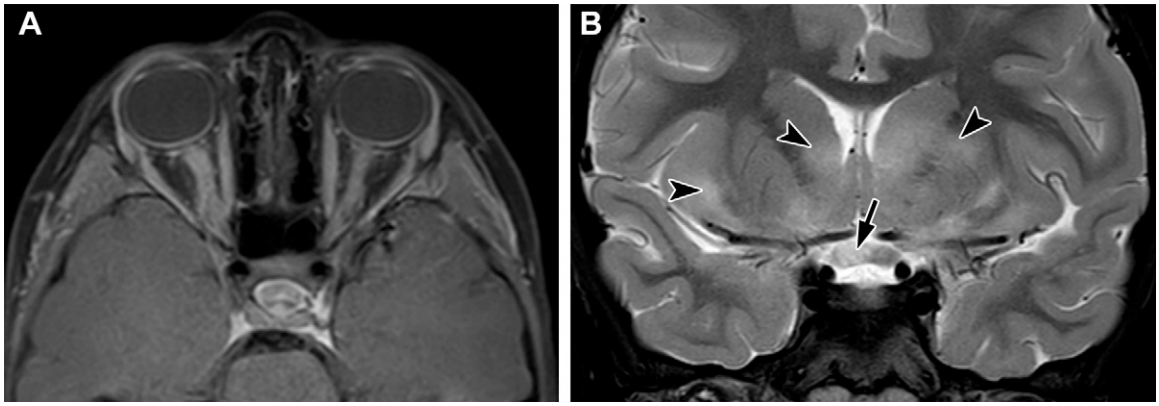

Figure 5. Myelin oligodendrocyte glycoprotein antibody–associated disease in a pediatric patient. **(A)** Axial contrast-enhanced T1W FS MR image of the orbits shows bilateral long-segment enhancement of the intraorbital ONs. **(B)** Coronal T2W MR image reveals increased T2 signal intensity and expansion of the optic chiasm (arrow) and multifocal T2-hyperintense foci scattered throughout the deep gray nuclei and subcortical white matter (arrowheads).

Sinonasal Disease

Acute Rhinosinusitis.—Acute rhinosinusitis (ARS) clinically manifests with fever, rhinorrhea, nasal congestion and/or drainage, and headache with a duration of 12 weeks or shorter (19). Viral ARS is most common (~90% of cases); however, bacterial superinfection can develop with sinus obstruction due to sinus outflow tract blockage (20).

ARS is diagnosed clinically, with imaging reserved for suspected orbital or intracranial complications (21). CECT is the modality of choice, given its availability, speed, and excellent depiction of bone detail. Fluid levels and bubbly secretions may be suggestive; however, these findings are nonspecific, as they often also occur in asymptomatic patients, and clinical correlation is needed. MRI is useful for identifying bone marrow edema and assessing for intracranial complications such as dural venous sinus thrombosis, epidural abscess, subdural empyema, meningitis, cerebritis, and cerebral abscess (Fig 6) (7,22). In atypical cases, MRI can help distinguish ARS from tumors such as leukemia, lymphoma, or rhabdomyosarcoma.

The term *Pott puffy tumor* describes subperiosteal phlegmon or abscess formation in the soft tissues overlying the frontal sinus (Fig 6). This term is a misnomer, as this process is infectious rather than neoplastic. Pott puffy tumor occurs in adolescents after pneumatization of the frontal sinus and is important to recognize given the high risk of associated intracranial

Table 3: Most Common Optic Neuritis MRI Characteristics of Pediatric Demyelinating Diseases

Disease	Location	Length	Laterality
Multiple sclerosis	Intraorbital	Short	Unilateral
MOGAD	Anterior, intraorbital	Long	Bilateral
Neuromyelitis optica	Posterior (with or without chiasm and tracts)	Long	Bilateral

Sources.—References 17 and 18.
Note.—MOGAD = myelin oligodendrocyte glycoprotein antibody–associated disease.

Figure 6. Pott puffy tumor (inflammation from acute frontal rhinosinusitis) in a 10-year-old girl. Sagittal T2W FS MR image shows frontal (*) and ethmoidal sinusitis, T2-hyperintense frontal subgaleal effusion, and a small T2-hypointense subperiosteal abscess (arrow).

complications in up to 50%–75% of pediatric patients (23,24). Treatments include broad-spectrum antibiotics and surgical drainage, including paranasal sinus decompression.

Acute Invasive Fungal Rhinosinusitis.—Acute invasive fungal rhinosinusitis (AIFR) is a dangerous and rapidly progressive infection that spreads through the mucosa into adjacent bone, soft tissues, orbits, and the intracranial compartment over a period of hours to days. Associated mortality rates have reached 40%–50% (25,26). Affected patients are usually immunocompromised, often from poorly controlled diabetes, hematologic malignancy, or immunosuppressive therapy (26). The majority of cases of AIFR are caused by *Aspergillus* species infection, though in individuals with diabetes, *Mucor* species and similar zygomycotic entities predominate (25,27). The clinical presentation includes persistent fever and congestion refractory to antibiotics, although headache, orbital symptoms, and cranial nerve palsies are possible. Endoscopy may show mucosal discoloration, decreased bleeding, and ulceration (25).

CECT and MRI are complementary, and both may be necessary for comprehensive bone and soft-tissue evaluation in cases of AIFR (28). CT demonstrates opacification of the affected sinus. Erosion of the sinonasal walls and/or nasal septum is a specific but not sensitive finding, as fungal spread often occurs through vascular channels of intact bone (27). There are typically inflammatory changes in the adjacent fat and decreased mucosal enhancement connoting ischemia and necrosis. MRI is superior for assessing soft-tissue and intracranial extension of disease, which is identified by a loss of normal T1-hyperintense fat signal in the premaxillary, retromaxillary, pterygopalatine, and intraorbital soft tissues (Fig 7). Postcontrast T1-weighted (T1W) fat-suppressed (FS) MRI may show reduced mucosal enhancement (ie, black turbinate sign) resulting from fungal invasion and tissue necrosis (Fig 7) (29). Restricted diffusivity has also been reported (30). Of note, the T2-hypointense signal of fungal elements typically seen with allergic fungal sinusitis is unusual with AIFR. MR or CT angiography and MR or CT venography are useful for assessment of mycotic aneurysm, arterial stenosis, and venous sinus thrombosis.

The differential diagnosis for AIFR includes infectious or inflammatory sinus diseases, as well as sinonasal malignancies. Treatment consists of aggressive surgical debridement, antifungal therapy, and addressing the underlying causes of the immunocompromise.

Juvenile Nasopharyngeal Angiofibroma.—Juvenile nasopharyngeal angiofibroma (JNA) is a benign locally aggressive vascular neoplasm that almost exclusively affects teenage males (31). The mass arises in the posterior nasal cavity at the sphenopalatine foramen, with frequent spread into adjacent spaces, including the pterygopalatine fossa, sphenoid sinuses, orbits, and infratemporal fossa (32). Large tumors may extend into the anterior or middle cranial fossa or central skull base (33). JNA presents clinically with nasal congestion and epistaxis and may progress to altered phonation, cranial nerve palsies, and proptosis.

Imaging of JNA reveals a well-marginated soft-tissue mass centered at the sphenopalatine foramen (Fig 8). CT shows bony remodeling or erosion and bowing of apposed osseous walls, while MRI reveals a mass with enlarged flow voids and T2-hypointense signal due to fibrous stroma. The avid postcontrast enhancement is related to the highly vascular nature of the lesion (Fig 8) (33). CT angiography and MR angiography show enlarged ipsilateral external carotid and internal maxillary arteries. The tumor may be supplied by the ascending

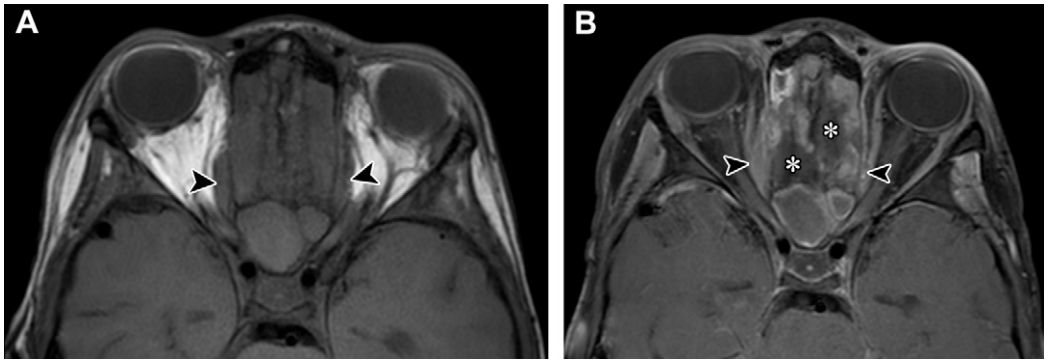

Figure 7. Acute invasive fungal rhinosinusitis in an 8-year-old boy with a history of orthotopic heart transplant, lymphoma, and Epstein-Barr virus infection who presented with a fever and nausea. Axial T1W **(A)** and contrast-enhanced T1W FS **(B)** MR images show extension of T1-hypointense, enhancing tissue through the lamina papyracea into the medial orbits (arrowheads). The postcontrast image shows the "black turbinate" sign (*), nonenhancing necrotic tissue from fungal invasion.

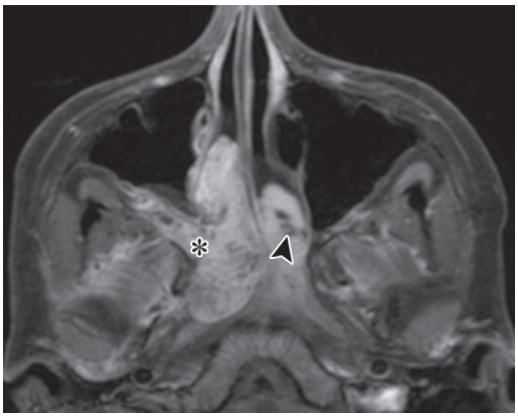

Figure 8. Juvenile nasopharyngeal angiofibroma in a 14-year-old adolescent boy with epistaxis and congestion. Axial contrast-enhanced T1W FS MR image shows an avidly enhancing nasopharyngeal mass centered at the sphenopalatine foramen (*), with internal flow voids (arrowhead).

pharyngeal artery, a branch of the internal maxillary artery. Digital subtraction angiography is the reference standard for clearly defining the arterial supply and is often indicated for presurgical embolization, which decreases bleeding complications (32). Biopsy is generally avoided, and, thus, accurate imaging diagnosis is critical (31).

The differential diagnosis for JNA includes rhabdomyosarcoma, nasopharyngeal carcinoma, lymphoma, and esthesioneuroblastoma. Noting the characteristic posterior nasal location, intense enhancement, and flow voids in a teenaged male patient is key to making an accurate diagnosis (31,32).

Oral Cavity and Aerodigestive Tract Disease

Foreign Bodies

Foreign bodies can be ingested, inhaled, or inserted into orifices such as the nares and external auditory canal. Both the location and the type of foreign body are important for radiologists to identify, especially since increasingly available magnets and button batteries may cause greater mechanical or chemical tissue damage than bland foreign bodies (eg, food, coins, and small toys). Children younger than 5 years or with developmental delays may be at higher risk (34,35).

Clinical presentations may be nonspecific and sometimes delayed in preverbal or neurodivergent children and include recurrent epistaxis, pain, respiratory distress, dysphagia, irritability, feeding difficulty, and coughing. The incident is often not witnessed.

Imaging is performed when a foreign body is suspected but not completely visualized at direct inspection, or if there is concern for complication. Anteroposterior and lateral neck radiographs are usually obtained first, acknowledging that some foreign bodies (eg, wood, food, or cloth) may be radiographically occult. Low-dose CT is helpful for troubleshooting, as most foreign bodies are well visualized. Correlation with the expected attenuation of the suspected foreign body is essential for sensitive interpretation.

Differentiating between a coin and a button battery is one of the radiologist's most important tasks. Ingested coins are typically managed nonoperatively, while button batteries require immediate removal to prevent a potentially catastrophic caustic mucosal injury that can occur in as little as 1–2 hours (36). Although similar in size to a coin, a button battery has a distinctive "double-ring" appearance on frontal radiographs and a "beveled-edge" appearance on lateral radiographs (Fig 9). Serial MRI with and without IV contrast material and MR or CT angiography may be indicated for complications such as tracheoesophageal fistula, vascular injury, and spondylodiscitis (37,38).

Odontogenic Infection

Complicated odontogenic infection is a common emergent head and neck condition in both adults and children, with similar clinical and imaging features between these patient groups. In the emergency setting, the first-line imaging examination for suspected complicated odontogenic infection is CECT. Dental caries appears as a rounded area of lucency along the tooth surface. Gingivitis may lead to periodontal disease and eventually periapical abscesses, which appear as areas of lucency in the maxillary or mandibular alveolar ridges adjacent to the tooth roots (39). Complications include cellulitis and subperiosteal or soft-tissue abscesses (which

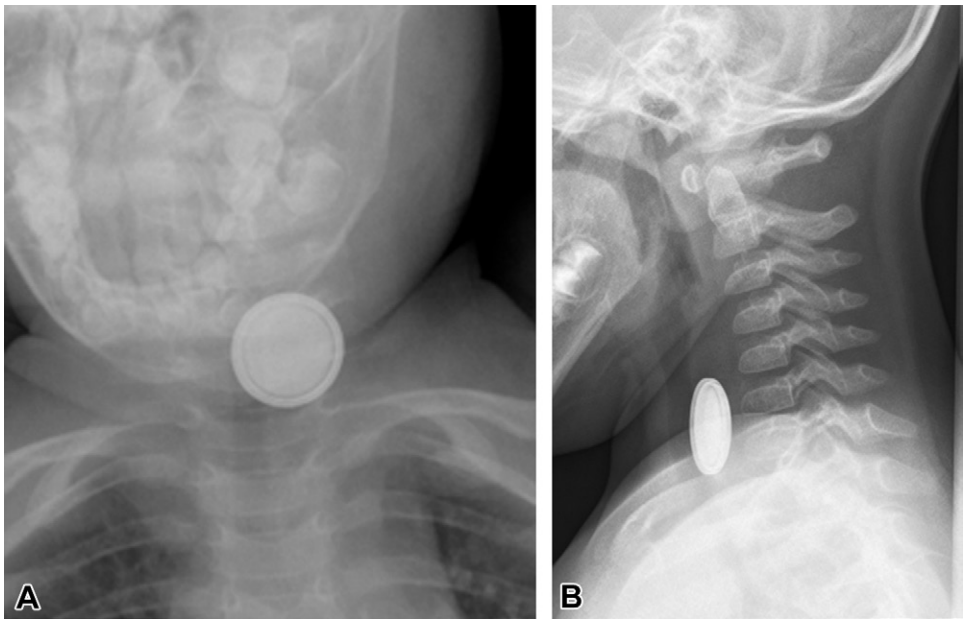

Figure 9. Recently ingested button battery in a pediatric patient. **(A)** Anteroposterior neck radiograph shows a double-ring appearance of the ingested button battery. **(B)** Lateral radiograph shows a beveled-edge appearance of the button battery. The location of the battery in the upper esophagus can be inferred by the round appearance of the battery in the anteroposterior projection and by the air-filled trachea observed to the right and in front of the foreign body.

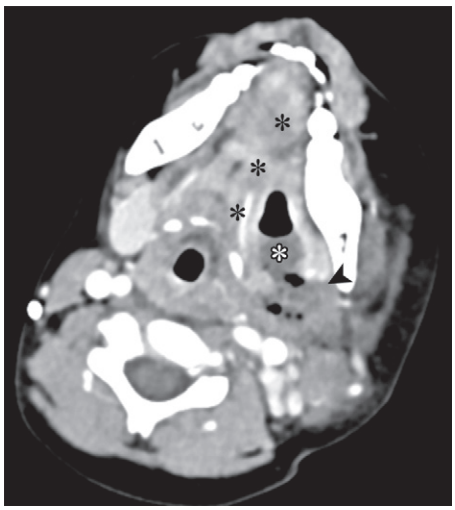

Figure 10. Ludwig angina in a 4-year-old girl with a fever and sore throat following a recent fall, during which she bit her tongue. Axial CECT image shows a gas- and fluid-containing abscess (white ∗) on the left side of the mouth floor. Note the fat stranding and phlegmon involving the sublingual (black ∗) and submandibular (arrowhead) spaces.

may extend into the deep neck compartments), osteomyelitis, and Ludwig angina.

Emergent Floor-of-the-Mouth Conditions

Ludwig Angina.—Ludwig angina is a rapidly progressive floor-of-mouth cellulitis with potential for rapid airway compromise resulting from displacement of the tongue into the pharyngeal airway. Odontogenic infection is the most common cause and typically involves the second and third mandibular molars whose root apices extend below the mandibular mylohyoid insertion (7,34). Oral trauma is an alternative cause. Patients present with pain, swelling, fever, and dysphagia.

CECT shows phlegmon or an abscess extending across the mylohyoid muscle to involve the submandibular and sublingual spaces (Fig 10) (7,34,40). Imaging evaluation includes assessment of airway patency and identification of a drainable abscess and/or underlying dental infections. Complications include mandibular osteomyelitis, spreading deep neck space infection, and Lemierre syndrome (internal jugular thrombophlebitis). Management includes airway control, antibiotics, and surgical decompression (7).

Angioedema.—Angioedema is transient soft-tissue swelling due to interstitial edema, most commonly affecting the face, tongue, lips, and larynx. Causes include allergic and hypersensitivity reactions, hereditary disorders such as C1 esterase inhibitor deficiency, and less commonly viral and bacterial infections. Although angioedema is often self-limiting and benign, rapidly progressive airway obstruction may be fatal (41). Angioedema is primarily a clinical diagnosis; however, imaging may be needed to distinguish it from disease processes that have overlapping clinical findings (42). On CT images, facial and neck swelling is usually diffuse and symmetric, with infiltrative trans-spatial edema, although findings may be asymmetric and focal (Fig 11) (42). Tongue enlargement is common.

Tonsillitis and Complications

Most cases of pediatric pharyngitis are viral and self-limiting. The most common treatable cause is group A *Streptococcus* infection. Symptoms and signs may include fever, throat pain, and tonsillar or pharyngeal exudates. Additional symptoms in patients with abscesses may include voice changes, drooling, and trismus. Uvular deviation, ipsilateral tonsillar bulging, or a neck mass may be found at physical examination (43).

CECT of the neck in select cases is primarily used to assess for drainable peritonsillar abscess or identify alternative

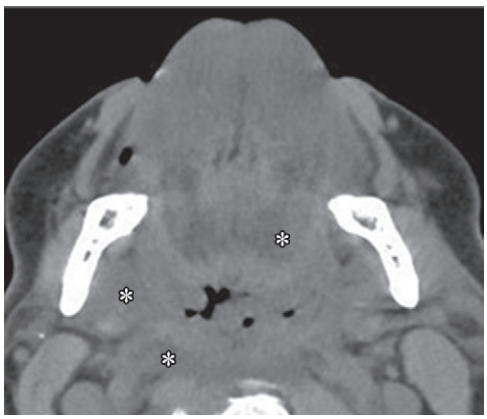

Figure 11. Acute-onset tongue swelling resulting from angioedema in a 14-year-old adolescent girl. Axial noncontrast CT image shows trans-spatial edema (∗) involving the sublingual, submandibular, parapharyngeal, and retropharyngeal spaces and resulting in marked narrowing of the airway. Intramuscular edema within the tongue contributes to the tongue protrusion.

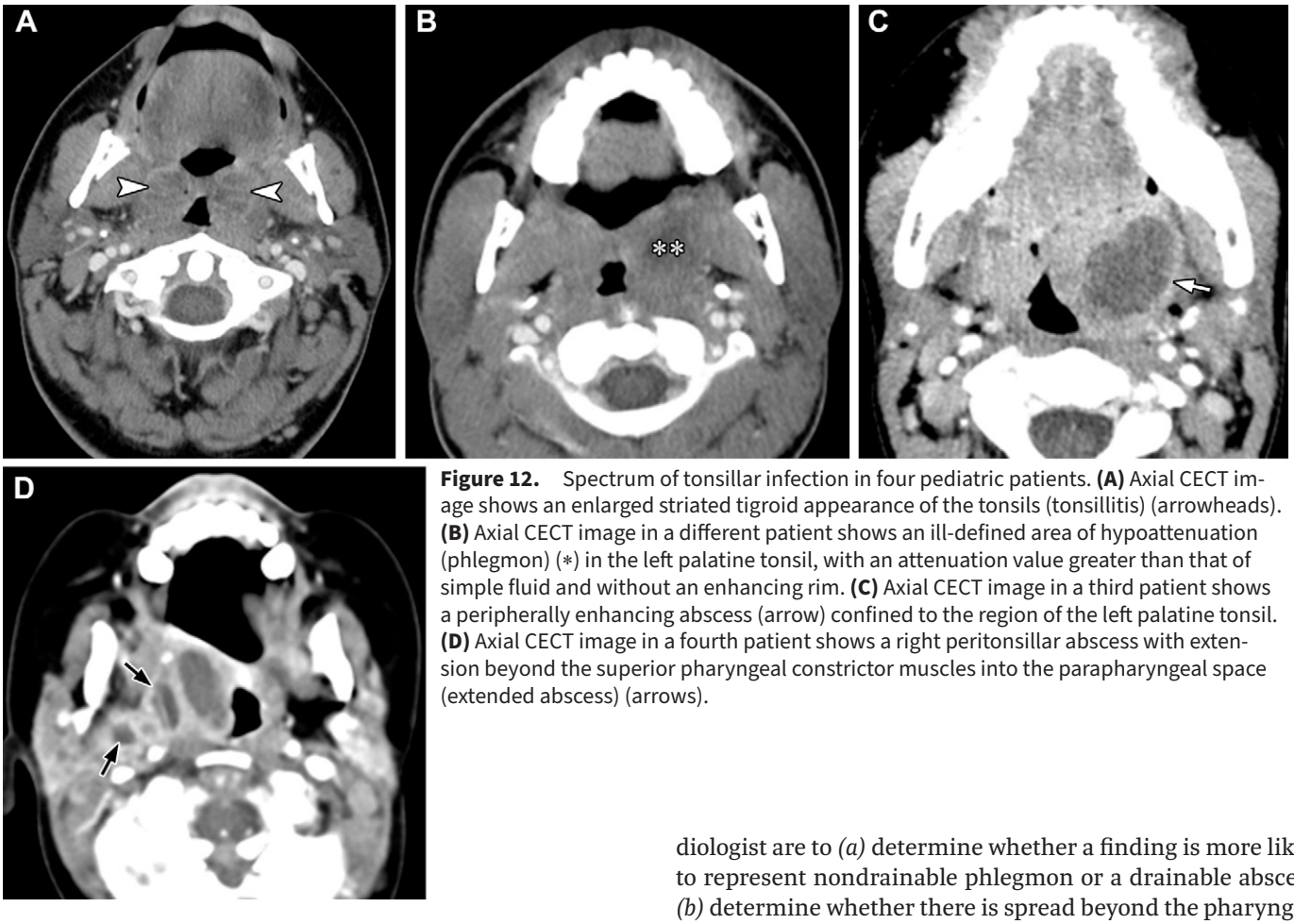

Figure 12. Spectrum of tonsillar infection in four pediatric patients. **(A)** Axial CECT image shows an enlarged striated tigroid appearance of the tonsils (tonsillitis) (arrowheads). **(B)** Axial CECT image in a different patient shows an ill-defined area of hypoattenuation (phlegmon) (∗) in the left palatine tonsil, with an attenuation value greater than that of simple fluid and without an enhancing rim. **(C)** Axial CECT image in a third patient shows a peripherally enhancing abscess (arrow) confined to the region of the left palatine tonsil. **(D)** Axial CECT image in a fourth patient shows a right peritonsillar abscess with extension beyond the superior pharyngeal constrictor muscles into the parapharyngeal space (extended abscess) (arrows).

causes such as retropharyngeal lymphadenitis or abscess. On CECT images, acute tonsillitis has a striated "tigroid" appearance of alternating enhancing and hypoattenuating tissue (Fig 12). Tonsillar phlegmon (nondrainable) appears as an ill-defined area of low attenuation (higher than the attenuation of water) without a well-defined enhancing rim (Fig 12).

Peritonsillar abscesses (between the tonsillar capsule and pharyngeal constrictor muscles) are much more common than intratonsillar abscesses (44,45). Although much attention is often devoted to distinguishing between intratonsillar and peritonsillar abscesses, this differentiation is generally of secondary importance. The more important roles of the radiologist are to *(a)* determine whether a finding is more likely to represent nondrainable phlegmon or a drainable abscess; *(b)* determine whether there is spread beyond the pharyngeal constrictors into adjacent anatomic spaces such as the parapharyngeal, masticator, and submandibular spaces (extended abscess); and *(c)* identify surgically relevant anatomy (eg, medialized retropharyngeal position of the internal carotid artery). Extended abscesses may cause greater mass effect on the airway and require more extensive surgical debridement. At CECT, a drainable peritonsillar abscess is more likely than phlegmon to have a well-defined enhancing rim and central water isoattenuation (Fig 12). However, it is important to note that while CECT is highly sensitive, it has a positive predictive value of around 83% (46). Therefore, some cases that appear to represent abscesses on CT images may not actually be drainable.

Table 4: Imaging Considerations for Emergent Upper Airway Infections in Pediatric Patients

Disease	Demographic Features and Cause	Clinical Considerations	Imaging Considerations
Croup (laryngotracheobronchitis)	Most common between 6 months and 3 years Upper airway obstruction, most often viral (eg, parainfluenza)	Presentation: viral prodome, fever, inspiratory stridor, "barking" or seal-like cough Treatment: oral or inhaled corticosteroids, intubation or hospital admission (only if severe)	Imaging to differentiate from foreign body ingestion or aspiration, other differential diagnoses Anteroposterior radiograph shows loss of normal shouldering (subglottic airway "steeple" sign); lateral radiograph shows subglottic narrowing, hypopharynx distention ("ballooned" hypopharynx) Radiographs are normal in ~50% of cases
Bacterial tracheitis (pseudomembranous croup, exudative tracheitis)	Rare alternative diagnosis to croup Affects patients aged 3–8 years Purulent tracheal infection with thick exudative airway plaques that slough Most common pathogen is *S aureus*	Presentation: rapid-onset respiratory distress with high fever and cough, often following viral prodrome Treatment: bronchoscopy and membrane stripping, possible intubation, intravenous antibiotics Fails to respond to steroids	Radiography shows subglottic airway linear filling defects, plaquelike irregularity with loss of parallel wall contours ("candle dripping" sign), indistinct air column; findings are similar to those of croup, but patients are older
Acute epiglottitis	Epiglottic or supraglottic inflammation Usually viral or bacterial infection Most common pathogen was previously *Haemophilus influenzae* type B, but is now non-typeable *H influenzae* Now (in vaccine era), older patients (adolescents) are more likely to be affected	Alternative causes: caustic exposure, anaphylaxis, angioedema Presentation: fever, drooling, respiratory distress, muffled "hot potato" voice Obtaining or maintaining airway is top clinical priority	Lateral radiography shows thickened epiglottis ("thumb" sign), aryepiglottic folds, airway narrowing, hypopharyngeal distention Beware of false epiglottic thickening on lateral neck radiograph in a rotated patient CT used only for differentiating acute epiglottitis from other conditions in stable patients with a well-controlled airway

Sources.—References 34, 46, and 47.

Tonsillitis and tonsillar phlegmon are treated with antibiotics and expectant management, with imaging indicated in refractory cases. Peritonsillar abscess may be treated with intravenous antibiotics. If there is an extended abscess or airway compromise, incision and drainage are also performed.

Upper Airway Infections

Important upper airway infections that may be encountered by radiology trainees on call include croup (laryngotracheobronchitis), bacterial tracheitis, and acute epiglottitis (Table 4) (Fig S3) (34,47,48). Imaging is generally of secondary importance to clinical findings, and radiography is the first-line modality for this group of disorders.

Sialadenitis

Sialadenitis, or salivary gland inflammation, typically presents with sudden-onset pain and swelling. Viral infections (eg, paramyxovirus) are the most common etiology for pediatric patients and are usually bilateral, with mumps-related sialadenitis now far less common due to widespread vaccination (49). *Staphylococcus aureus* and *Streptococccus* species are the most common bacterial pathogens, with infection occurring due to salivary stasis with ascending bacterial infection (50). Bacterial infection is more often unilateral. Sialolithiasis is uncommon in children and seen most often with submandibular sialadenitis. Recent surgery, Sjögren syndrome, diabetes, hypothyroidism, renal failure, radiation therapy, chemotherapy, and dehydration cause predisposition to developing sialadenitis due to reduced salivary secretion (50).

Although imaging is not necessary for the diagnosis, it is often performed to evaluate for complications such as abscess and alternative diagnoses such as a mass or lymphadenitis. US can show glandular enlargement and hyperemia (Fig 13). CT and MRI can reveal an enlarged, hyperenhancing gland with surrounding edema (50). First branchial apparatus anomalies (BAA) may involve the parotid region and may be suspected in cases of recurrent infection. A calculus with associated ductal dilatation may be seen uncommonly (Fig 13). Treatment is generally supportive, although antibiotics are indicated for cases of a suspected bacterial cause.

Neck Disease

Suppurative Lymphadenitis, Retropharyngeal Abscess, and Lemierre Syndrome.—Pediatric cervical lymph nodes are normally larger than those seen in adults, even in asymptomatic children. *Streptococcus*-related pharyngitis and Epstein-Barr virus infection may cause striking bilateral cervical lymphadenopathy and adenoid inflammation.

Suppurative lymphadenitis (complicated by nodal abscesses) results from nodal bacterial infection, is most commonly

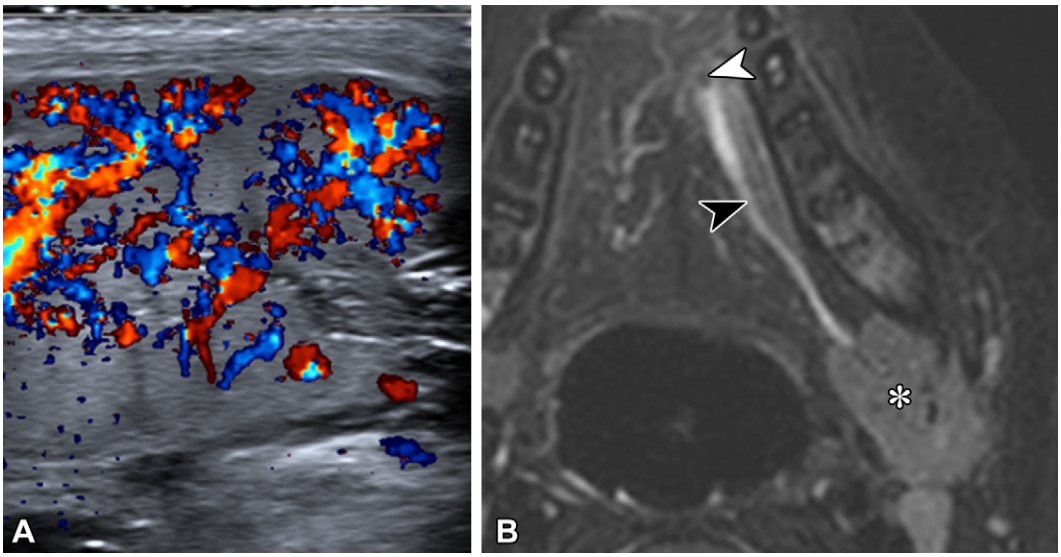

Figure 13. Sialadenitis in two pediatric patients. **(A)** Transverse color Doppler US image in a 6-year-old boy with neck swelling shows an enlarged, heterogeneous, hyperemic submandibular gland. **(B)** Axial T2W FS MR image in a 7-year-old boy with recurrent pain and swelling under the tongue shows a mildly edematous left submandibular gland (*) and dilatation of the Wharton duct (black arrowhead) secondary to an obstructive calculus (white arrowhead). Sialadenitis due to obstructing calculus is rarer in children than in adults.

due to *Staphylococcus* or *Streptococcus* species infection, and often follows a primary head and neck infection (eg, tonsillitis) (51). Patients may present with fluctuant neck swelling with erythema and fever. US reveals enlarged hypervascular, sometimes heterogeneous lymph nodes and surrounding fat hyperechogenicity due to cellulitis. Sonography may help to differentiate abscess from nondrainable phlegmon, while CECT is useful for detection and troubleshooting in cases of deep or extensive abscess. Lateral retropharyngeal node (of Rouvière) involvement is common and often mistaken for peritonsillar abscess or retropharyngeal or parapharyngeal abscess. Suppurative retropharyngeal lymphadenitis is centered more posterosuperiorly than tonsillar abscess and is distinguished from retropharyngeal abscess by confinement within the lymph node. The latter distinction is clinically relevant, as the management of these entities differs.

Suppurative retropharyngeal lymphadenitis can be complicated by rupture of the nodal abscess into the retropharyngeal space. At CECT, the resultant retropharyngeal abscess has convex borders and peripheral enhancement ("football" shaped) in contradistinction to reactive retropharyngeal effusion, which has a "bow tie" shape and no peripheral enhancement (Fig 14) (52). This distinction is important, as abscesses are surgically drained, while effusions are not. Retropharyngeal abscesses may extend to the skull base superiorly and the cervicothoracic junction inferiorly. Importantly, if a retropharyngeal infection spills over into the adjacent danger space, infection can spread to the mediastinum and prevertebral soft tissues (Fig 14). This phenomenon can be life threatening, leading to rapidly progressive airway compromise or thoracic infection.

Reactive retropharyngeal effusions can be seen due to numerous underlying infectious or inflammatory causes, including Kawasaki disease (along with cervical lymphadenopathy). Longus colli calcific tendinitis is a rare cause in children.

Vascular complications of suppurative lymphadenitis may include internal jugular thrombophlebitis and resultant septic emboli, most commonly to the lungs (Lemierre syndrome, most often due to *Fusobacterium necrophorum* [Fig 15]). It is important to note that clinically insignificant effacement is more common than thrombosis in this context (53). Self-limiting internal carotid arterial inflammation may occur.

The differential diagnosis for suppurative lymphadenitis includes nontuberculous mycobacterial infection, which tends to present subacutely in relatively healthy toddlers with lymphadenitis refractory to antibiotics. In this condition, the affected node(s) may be calcified and tend to fistulize to the skin, with relatively little surrounding cellulitis (Fig S4) (54). *Bartonella henselae* infection may also cause more indolent, striking nodal enlargement and necrosis refractory to first-line antibiotic therapy. Metastatic lymph nodes (especially from thyroid carcinoma) are an additional differential consideration but are less likely to present in acute settings. Notably, these nodes may be calcified, hyperenhancing, or cystic in appearance.

Infected Congenital Cysts.—The most common infected congenital cervical cysts and associated malformations include branchial apparatus anomalies, thyroglossal duct cysts, and dermoid inclusion cysts (Fig 16, Table 5) (55,56). Location is of key importance in distinguishing among these entities, given their overlapping clinical and imaging findings. US and CT have complementary roles in emergency settings, while MRI is most helpful after the subsidence of acute inflammation. Sonographic findings include internal debris, sometimes with a "pseudosolid" appearance; wall thickening and rim enhancement; and surrounding inflammatory fat stranding and hypervascularity. The main differential considerations include suppurative lymphadenitis, infected lymphatic malformations, cystic or necrotic tumors, and sialoceles.

Vascular Conditions

Vascular Malformations

Vascular malformations are congenital anomalies of vascular development. Nomenclature is based on the involved vessels, and lesions often involve multiple anatomic spaces (trans-spatial). While these malformations are present at birth, they occasionally present for the first time in the acute setting, usually in young children and because of complications.

Figure 14. Retropharyngeal infections in three pediatric patients. **(A)** Sagittal CECT image shows thin reactive retropharyngeal effusion (arrowhead) without a bulging contour or wall enhancement. **(B)** Axial CECT image in a different patient reveals a circumscribed hypoattenuating fluid collection (∗) contained within a lateral retropharyngeal node (ie, intranodal abscess). **(C, D)** Sagittal **(C)** and axial **(D)** CECT images in a third patient show a peripherally enhancing retropharyngeal abscess with convex borders (arrows in **C**) and multiple mediastinal abscesses (arrows in **D**).

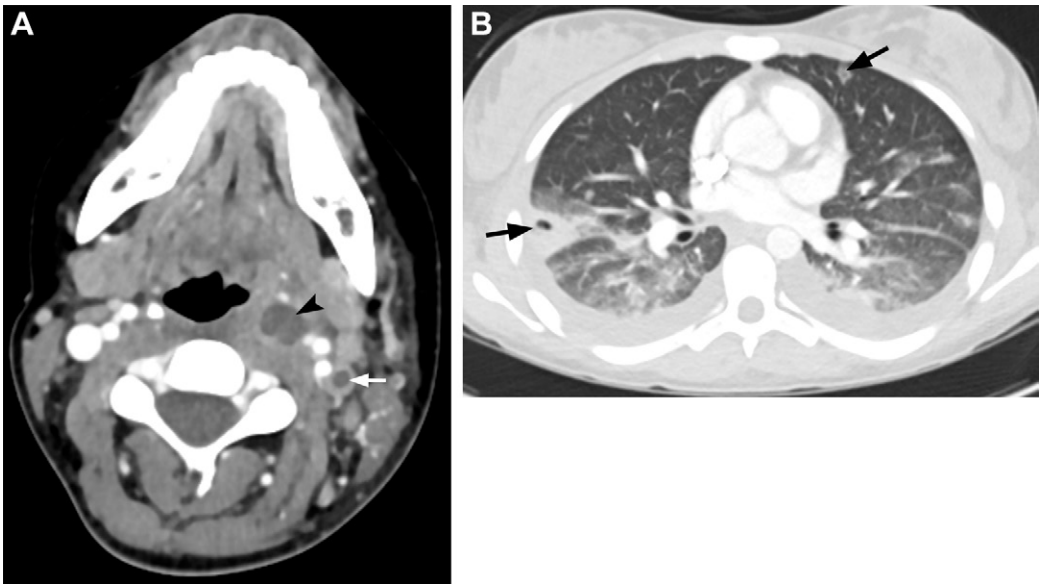

Figure 15. Peritonsillar abscess extending into the left parapharyngeal space complicated by Lemierre syndrome in a 17-year-old adolescent girl. **(A)** Axial CECT image shows a parapharyngeal space abscess (arrowhead) and nonocclusive hypoattenuating thrombus (arrow) in the left internal jugular vein. **(B)** Axial CT image (lung window) shows peripheral cavitary lung nodules (arrows). Lemierre syndrome can complicate any head and neck infection, and the radiologist is often the first to suspect the diagnosis.

Figure 16. Infected congenital cysts in two pediatric patients. **(A)** Sagittal contrast-enhanced T1W FS MR image in a 6-year-old boy with neck swelling shows a peripherally enhancing thyroglossal duct cyst (arrow) anterior to the hyoid, with surrounding inflammatory change. **(B)** Coronal CECT image in a 16-year-old adolescent boy with recurrent neck swelling shows an infected second branchial cleft cyst (∗) with an adjacent enhancing sinus tract (arrowheads).

Lymphatic malformations (LMs) comprise abnormally formed lymphatic channels and are classified as macrocystic (if the cystic components are larger than 1 cm) or microcystic. Macrocystic LMs appear as multiseptated cystic masses without internal vascular flow or solid enhancement (Fig 17). Fluid-fluid or hematocrit levels are common (57). LMs can present acutely as rapidly growing masses. If complicated by internal hemorrhage or infection, there may be debris within the cysts. Differentiating LMs from other fluid collections in the neck can be challenging; however, LMs tend to be trans-spatial, conform to surrounding structures, and are less likely to be unilocular than other congenital neck cysts. They also occur in locations beyond those typically encountered in common infections (tonsils, retropharyngeal space, subperiosteal) or classically located congenital lesions such as thyroglossal duct cysts and branchial apparatus anomalies.

Venous malformations consist of abnormal venous channels and can present acutely with symptoms of thrombophlebitis. Imaging reveals multiple cystic-appearing spaces with venous flow at Doppler US assessment and progressive "puddling" enhancement on CECT and MR images. Phleboliths are pathognomonic when present (Fig S5) (57). Thrombosed malformations may show little internal flow or enhancement and exhibit surrounding inflammatory changes.

Arteriovenous malformations are rare malformations defined by a nidus of vessels with an abnormal arteriovenous connection and without an associated soft-tissue mass. They may be complicated by acute hemorrhage.

Acute Arterial Abnormalities

Arterial Dissection.—Spontaneous or nontraumatic dissection may occur without trauma or following innocuous trauma (eg, minor sports-related impact), a history that is more common in the vertebrobasilar circulation than the carotid circulation (58). The feared consequence is cerebral ischemic injury, usually due to thromboembolism. Risk factors include connective tissue disorders (eg, Ehlers-Danlos syndrome), craniocervical junction osseous anomalies, cervical spine instability, and male sex (59). Nonspecific symptoms may include headache or neck pain.

In the emergent setting, patients are usually imaged with MR or CT angiography. For vertebral artery dissection, three-dimensional time-of-flight MR angiography of the neck in conjunction with stroke protocol brain MRI is a good initial choice for vascular imaging. Although T1W two-dimensional turbo spin-echo FS MRI is commonly performed to detect T1-hyperintense intraluminal thrombus, many potential technical pitfalls reduce the utility of this sequence on MR images of pediatric vertebral artery dissection (60). Findings of cervical dissection include stenosis or occlusion, a visible intimal flap (linear filing defect, rarely seen), intraluminal thrombus (a filling defect, often crescent shaped), or pseudoaneurysm (saccular bulging from the vessel wall) (Fig 18) (60). Carotid dissections are most common approximately 2–3 cm above the carotid bulb or near the C1-C2 cervical vertebra level (59). Vertebral dissections are most common at the V2-V3 vertebral segment junction or in the proximal V3 segments (60). Knowledge of normal anatomic variants such as arterial fenestration can be helpful.

Vasculitis.—Vasculitides such as Takayasu arteritis or infectious arteritis are caused by arterial wall inflammation. Takayasu arteritis, the most common large-vessel vasculitis in pediatric patients, is a granulomatous vasculitis that most commonly affects the aorta and its major branches. Affected patients present with transient ischemic attack or stroke, hypertension, dyspnea, fever, headaches, and/or weight loss.

Table 5: Imaging and Clinical Considerations in Infected Head and Neck Congenital Cysts

Condition	Definition	Location (Most Common)	Clinical Considerations	Imaging Considerations
BAA	Cysts, sinuses, or fistulas resulting from aberrant development of the branchial apparatus (embryonic precursor to numerous head and neck structures, with pouches, arches, clefts)	1st: ear or parotid region to submandibular space 2nd (most common): posterior to submandibular gland, anterior to sternocleidomastoid, lateral to carotid sheath; deep components may be at tonsillar fossa 3rd (rare): pyriform sinus sinus tract from mid-pyriform sinus, posterior cervical cyst 4th: pyriform sinus sinus tract from sinus apex	Lesions variably involve the mucosal surface of the aerodigestive tract, the neck soft tissues, and skin Most commonly present in young children with a tender mass, cellulitis, or skin drainage from a cutaneous pit	1st BAA may show low diffusivity (DWI) and simulate a dermoid or epidermoid cyst; look for middle or external ear cholesteatomas 2nd branchial apparatus cyst: beware of mimics (cystic nodal metastases in thyroid or squamous cell carcinoma in adolescents) 3rd and 4th BAA: consider in patients with recurrent thyroid infections
TGDC	Remnants of embryonic thyroglossal duct	Anywhere from foramen cecum (tongue base) to thyroid Most common at hyoid level, touching hyoid Suprahyoid and/or hyoid lesions at midline Infrahyoid lesions off-midline, closely related to strap muscles with "claw" sign	Presentation: midline or paramedian neck mass that moves with tongue protrusion, tenderness, cellulitis if infected Treatment: control of acute infection, Sistrunk procedure (area of hyoid contacting cyst must be resected)	US shows relationship with hyoid, strap muscles, and cystic nature of mass CT and MRI for troubleshooting Locate normal thyroid (only functioning tissue may be TGDC, leading to surgical implications)
Dermoid or epidermoid inclusion cysts	Inclusion cysts containing epithelial tissue: Squamous debris: epidermoid cyst If also dermal appendages: dermoid cyst Difficult to reliably distinguish from one another; hence, the common use of "dermoid/epidermoid"	Numerous locations, commonly along lines of sutural fusion (scalp or skull, brow, nasofrontal, retroauricular regions), oral cavity, or midline neck In the infrahyoid neck, more likely to be midline than TGDC, often in the suprasternal notch	Nasofrontal or skull-involving dermoid or dermal sinus tracts may have intracranial infectious complications	US or CT is usually sufficient for diagnosis, except for nasal dermoids with possible intracranial components that warrant MRI evaluation Dermoids are more likely to contain fat and calcification Epidermoid cysts may show low diffusivity (DWI)

Sources.—References 54 and 55.
Note.—BAA = branchial apparatus anomalies, DWI = diffusion-weighted imaging, TGDC = thyroglossal duct cyst.

Serum inflammatory markers may be elevated (61). Imaging findings include arterial stenosis, concentric wall thickening (with enhancement at vessel wall MRI), occlusion, aneurysms, or dissection (Fig 19).

Infectious arteritis may result from head and neck infections, including lymphadenitis and mastoiditis. The inflammed or narrowed arterial segment is seen adjacent to the primary infection. Although suppurative retropharyngeal lymphadenitis and abscess are frequently associated with self-limiting internal carotid artery narrowing, mycotic pseudoaneurysms associated with *Staphylococcus*, *Escherichia coli*, and *Salmonella* infections rarely may occur (62,63).

Temporal Bone and Skull Base Disease

Coalescent Otomastoiditis and Labyrinthitis.—Pediatric acute otomastoiditis commonly presents with ear pain, postauricular tenderness, and swelling and is managed nonsurgically. Imaging is reserved for patients who are toxic appearing, have symptoms concerning for complication, or have persistent symptoms despite having received appropriate antibiotic therapy (64).

CECT of the temporal bones is the imaging study of choice in the emergency setting, with MRI performed in cases with suspected intracranial complications. Coalescence is diagnosed when erosion of the mastoid septa and/or bony cortex occurs and distinguishes coalescent mastoiditis from simple mastoid effusion or "incipient mastoiditis," which is commonly seen with otitis media or even in asymptomatic patients (Fig 20).

In coalescent mastoiditis, there may be rim-enhancing abscesses within the mastoid. Depending on the location, cortical breach may result in superficial subperiosteal abscess, epidural abscess, and/or jugular or sigmoid sinus thrombosis (Fig 20). Differentiating an epidural abscess from clot in the adjacent sigmoid sinus can be difficult, but if fluid is seen uplifting an opacified dural venous sinus, an epidural collection

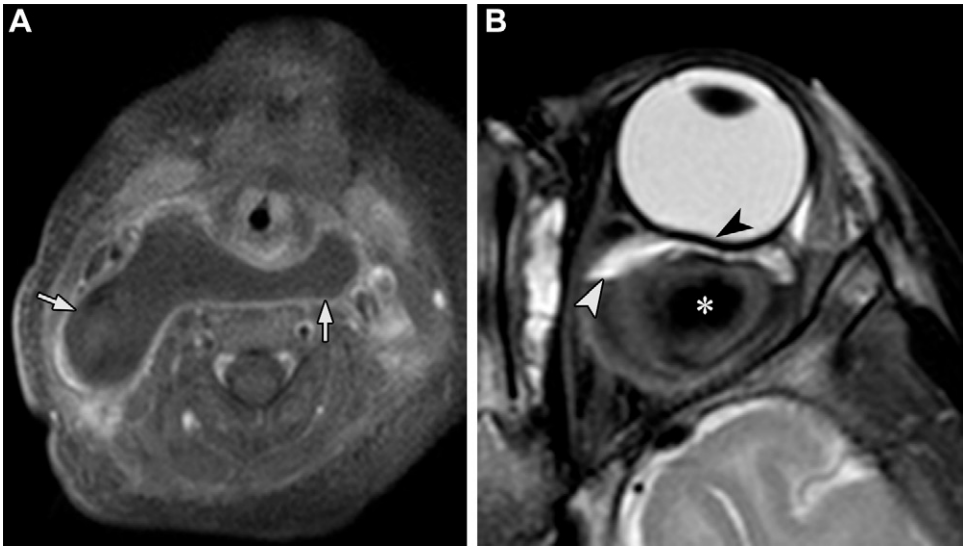

Figure 17. Complicated lymphatic malformations (LMs) in two pediatric patients. **(A)** Axial contrast-enhanced T1W FS MR image in a 14-month-old boy with a known LM and fever shows a large retropharyngeal LM with a thick rind of enhancement and surrounding cellulitis (arrows). **(B)** Axial T2W FS MR image in a 6-month-old boy with proptosis shows acute hemorrhage (*) within an intraorbital LM. Note the fluid-hemorrhage level (white arrowhead) and marked flattening of the posterior globe (black arrowhead).

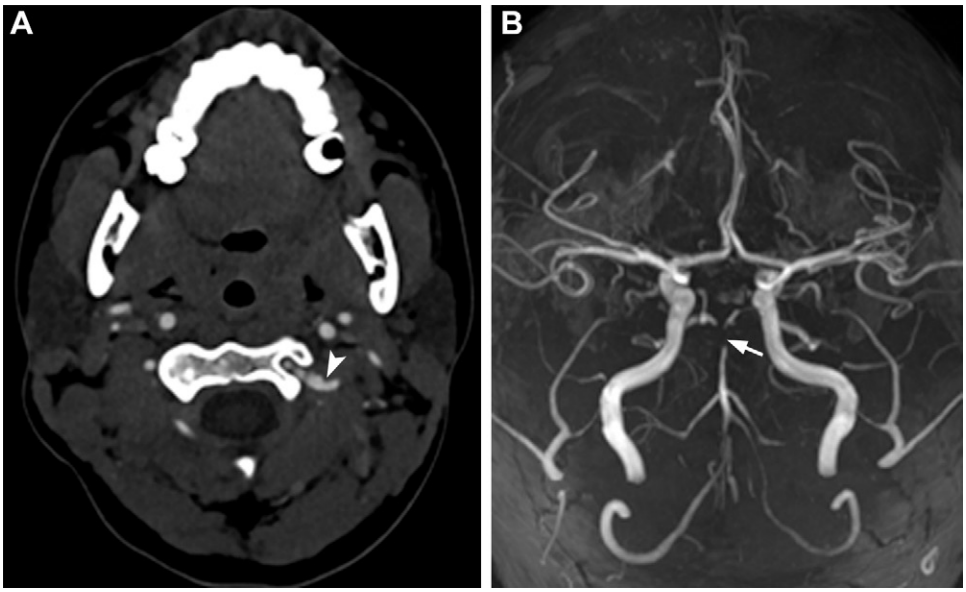

Figure 18. Vertebral artery dissection in a 16-year-old adolescent boy who presented with headache, dizzy spells, and vertigo. **(A)** Axial CT angiographic image of the neck shows focal irregularity and subtle narrowing of the left V3 vertebral artery segment (arrowhead). **(B)** Three-dimensional maximum intensity projection MR angiographic image of the circle of Willis shows a diminutive caliber of the left intracranial vertebral artery and basilar tip occlusion (arrow).

is likely present. Thrombus may have higher attenuation than an abscess. MRI may be helpful for differentiation in some cases, which may affect the surgical approach and the decision to anticoagulate. Meningitis, cerebritis, and parenchymal abscess may be seen with further intracranial involvement (Fig 20). Phlegmonous extension or abscess extending along the sternocleidomastoid muscle (Bezold abscess) is less common in pediatric patients due to incomplete pneumatization of the mastoid tip (65).

An important complication to look for on MR images is labyrinthine enhancement connoting acute labyrinthitis, which may lead to permanent hearing loss due to labyrinthitis ossificans if left untreated (Fig 21). Decreased vestibulocochlear T2 signal occurs subacutely, and mineralization detectable with CT occurs as a late finding (66). Labyrinthitis can also be seen as a complication of trauma, surgery, or meningitis, especially from an *S pneumoniae* or *H influenzae* infection.

Cholesteatoma, rhabdomyosarcoma, and Langerhans cell histiocytosis are important imaging differential diagnostic considerations, although patients with these conditions usually present less acutely and their imaging findings differ. Mastoidectomy and intravenous antibiotic therapy are the mainstays of treatment.

Petrous Apicitis.—Pneumatization of the petrous apex is a normal anatomic variant, and air cells commonly contain bland effusion (Fig 22). Petrous apicitis occurs when fluid-filled petrous apex air cells become superinfected. Osteomyelitis and lytic bone destruction may occur (Fig 23). Deep facial pain is the most common presenting symptom and is related to irritation of the adjacent trigeminal nerve in Meckel cave, although more advanced cases may also have abducens palsy (Gradenigo triad) or hearing loss (67).

On MR images, there is increased T2 and/or short-tau inversion-recovery signal intensity and enhancement of the petrous apex with or without abscess formation (Fig 23) (66). Complications include skull base osteomyelitis, cranial neuritis, dural venous and/or cavernous sinus thrombosis,

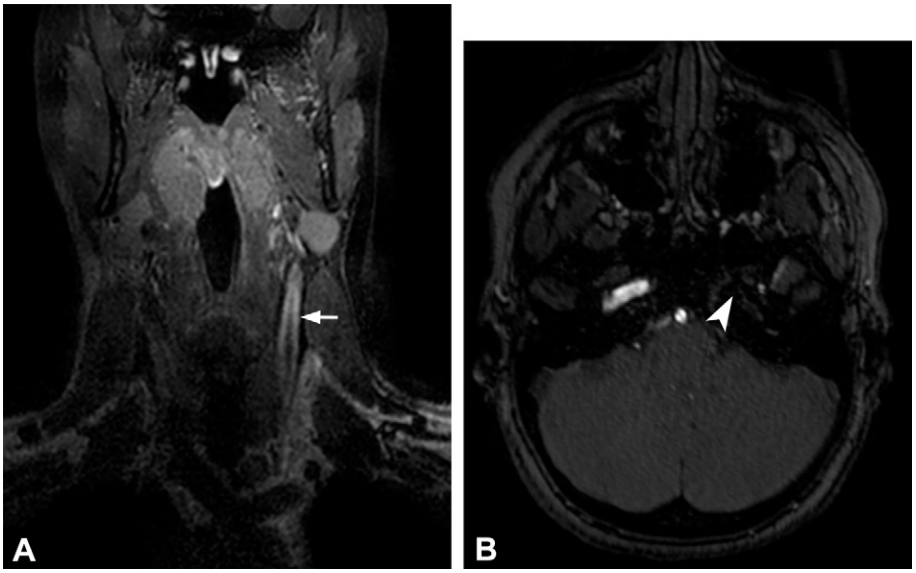

Figure 19. Takayasu arteritis subsequently diagnosed in a 15-year-old adolescent girl with episodic weakness. **(A)** Coronal contrast-enhanced T1W FS MR image of the vessel wall shows circumferential wall enhancement (arrow) of the common and internal carotid arteries. **(B)** Axial MR angiographic image reveals an absence of flow-related enhancement (arrowhead) in the left petrous internal carotid artery segment.

Figure 20. Imaging of the temporal bone in three pediatric patients. **(A)** Axial temporal bone CT image shows nonspecific mastoid and middle ear fluid in a 7-year-old boy with eustachian tube dysfunction. Note the intact mastoid septa and cortex. **(B)** Axial temporal bone CECT image in a 12-year-old boy shows coalescent mastoiditis with erosion of the mastoid septa and mastoid cortex (arrowheads) and overlying postauricular swelling (*). **(C)** Contrast-enhanced T1W FS MR image shows complicated otomastoiditis in a 4-year-old boy with ear pain, with jugular bulb and sigmoid venous sinus thrombus (white arrow), small epidural abscess (arrowhead), and subperiosteal abscess with surrounding cellulitis (black arrow).

meningitis, subdural or epidural abscess, and internal carotid artery arteritis and/or vasospasm.

Skull Base Osteomyelitis.—Skull base osteomyelitis (SBO) most commonly involves the temporal bone or basiocciput (68). Pediatric SBO is rare, typically arising as a direct complication of adjacent head and neck infection or rarely as a postsurgical complication (69). Clinical presentation is nonspecific, with symptoms such as headache and facial or neck pain. Cranial nerve palsies correspond to the location of the inflammation (68).

CECT is the initial study of choice based on convenience and superior ability to depict bone erosion and/or demineralization (Fig 24) (70). Further evaluation with MRI is often pursued to assess the full extent of skull base involvement (marrow and adjacent soft-tissue edema and enhancement) and intracranial complications, which are similar to those described with mastoiditis (70).

Destructive skull base neoplasms such as rhabdomyosarcoma, leukemia, metastatic neuroblastoma, and Langerhans cell histiocytosis are important differential considerations and can often be differentiated on the basis of the presence of enhancing soft-tissue masses.

Musculoskeletal Abnormalities

Fibromatosis Colli.—Fibromatosis colli is a posttraumatic, inflammatory, nonneoplastic process characterized by nontender enlargement of the sternocleidomastoid, which may result in torticollis. Presentation occurs within the first few weeks after birth, and the disorder regresses spontaneously or with physical therapy (71). Fibromatosis colli is most often

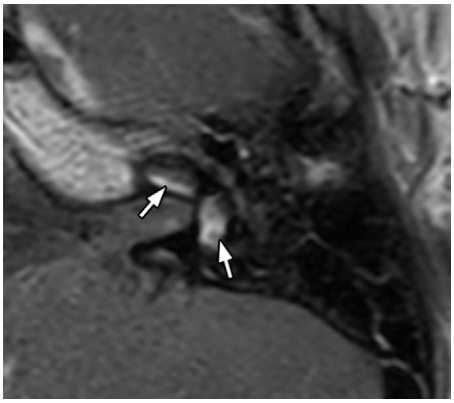

Figure 21. Axial contrast-enhanced T1W FS MR image in a 4-year-old girl with meningitis shows focal enhancement in the cochlear basal turn and vestibule (arrows) consistent with acute labyrinthitis.

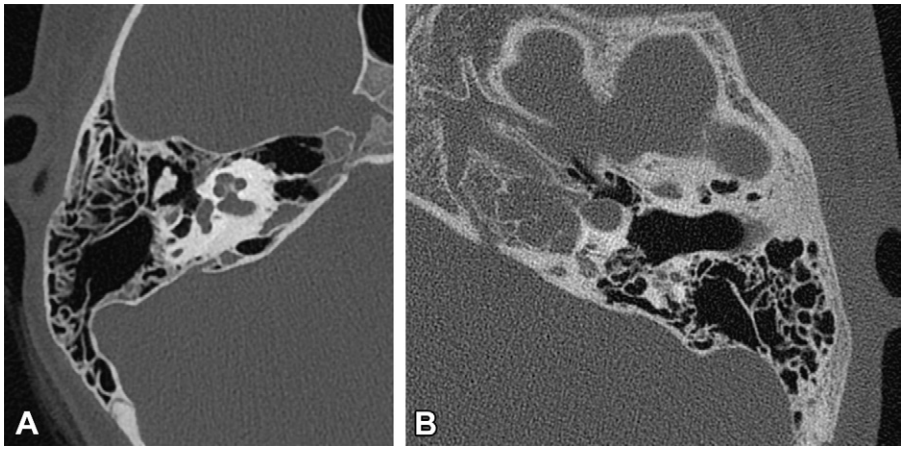

Figure 22. Axial temporal bone CT images demonstrate variations of the petrous apex in two different pediatric patients. **(A)** Pneumatized petrous apex. **(B)**Pneumatized petrous apex with opacified air cells due to bland effusion. Note the lack of expansion, intact cortex, and relatively hyperaerated mastoid.

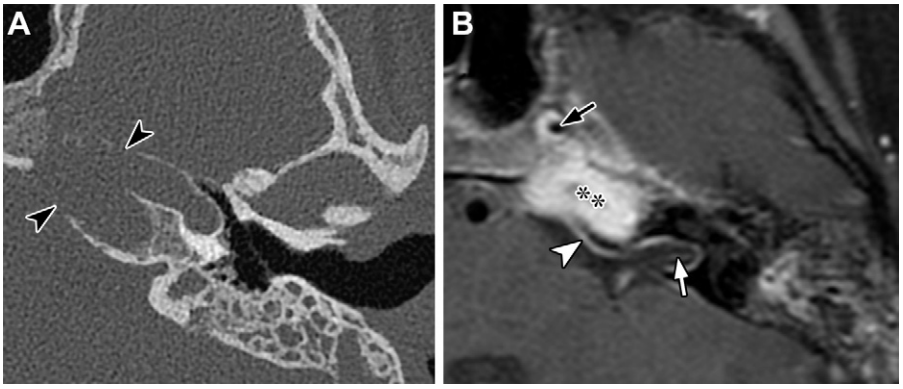

Figure 23. Petrous apicitis and the Gradenigo triad in a 13-year-old adolescent girl who presented with left lateral rectus palsy. **(A)** Axial temporal bone CT image shows cortical destruction of the petrous apex (arrowheads). **(B)** Axial contrast-enhanced T1W FS MR image shows extensive enhancing soft tissue and/or phlegmon in the petrous apex (*), vasospasm of the cavernous internal carotid artery (black arrow), meningeal enhancement (meningitis) (arrowhead), and abnormal cranial nerve enhancement in the internal auditory canal (white arrow).

unilateral, and a history of difficult delivery or breech presentation may be associated.

US is the diagnostic study of choice and shows fusiform enlargement of the sternocleidomastoid muscle body, with variable echogenicity and color Doppler flow depending on the acuity (Fig 25). Imaging of the contralateral neck for comparison is key. Similar findings in an older infant, particularly if new, may raise concern for neoplasm such as sarcoma. In fibromatosis colli, acute inflammation and regional nodal enlargement are notably absent.

Cervical Spine Abnormalities

Although a comprehensive discussion of cervical spinal abnormalities is beyond the scope of this article, Grisel syndrome and discitis-osteomyelitis are briefly discussed, as it is important for radiologists to consider these conditions that are often not clinically suspected at the time of initial imaging in children with acute neck pain.

Grisel syndrome is nontraumatic fixed atlantoaxial subluxation secondary to head and neck infection or inflammation, with the latter typically being postsurgical following adenotonsillectomy. Ligamentous laxity is believed to contribute to this subluxation, as most cases occur in pediatric patients and/or those with conditions predisposing to laxity (eg, trisomy 21 or Marfan syndrome) (72). The key imaging finding of Grisel syndrome is fixed rotation and/or subluxation of the C1 cervical vertebra on the C2 cervical vertebra (Fig 26). Follow-up or dynamic CT may be needed for confirmation. Accompanying

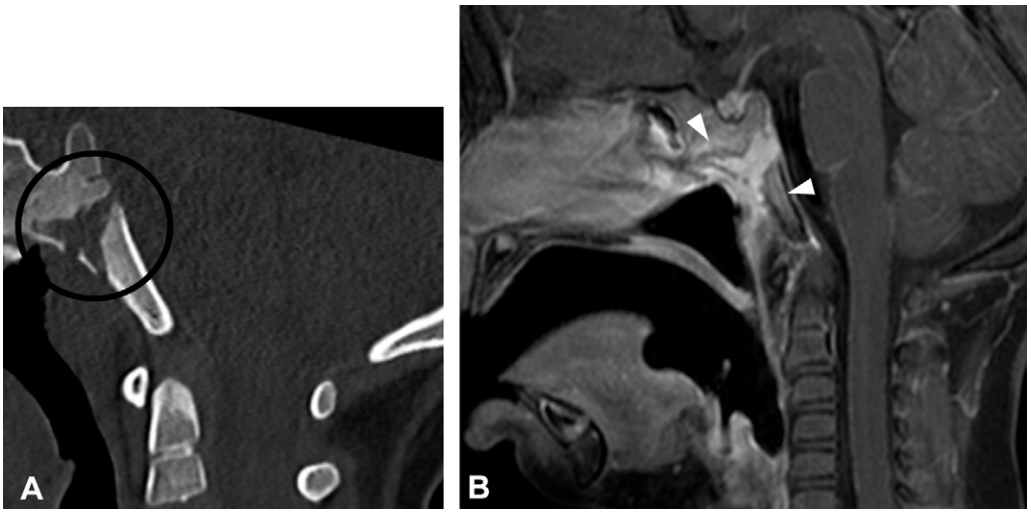

Figure 24. Spheno-occipital synchondrosis–related osteomyelitis diagnosed in a 3-year-old boy who presented with neck pain after adenoidectomy. **(A)** Sagittal CT image shows widening and irregularity of the spheno-occipital synchondrosis, with subtle marginal sclerosis (circle outline). **(B)** Sagittal contrast-enhanced T1W FS MR image shows enhancement in and widening of the synchondrosis and adjacent enhancement of the sphenoid body and basiocciput (arrowheads).

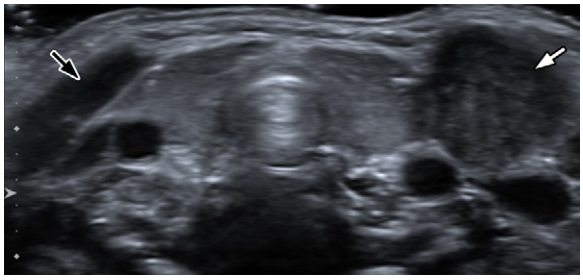

Figure 25. Neck mass in a 34-day-old boy. Transverse gray-scale neck US image shows unilateral fusiform enlargement and a mildly heterogeneous echotexture in the left sternocleidomastoid muscle (white arrow) compared with the normal right side (black arrow).

suppurative lymphadenitis, tonsillitis, retropharyngeal infection, or otomastoiditis should be sought as causal factors. Treatment includes reduction and immobilization. Surgery may be required if the condition is not treated early.

Discitis-osteomyelitis is a suppurative infection of the intervertebral disk and adjacent vertebral bodies that usually occurs due to hematogeneous spread and less often as a traumatic or surgical complication. The most common causal pathogen is methicillin-resistant *S aureus* (73). Cervical discitis-osteomyelitis is rare, and nonspecific clinical signs and symptoms often lead to a delayed diagnosis. Radiography and CT may show a loss of intervertebral disk space height or endplate irregularity, although they may be normal (74). MRI is more sensitive, particularly early in the disease course, showing disk edema, marrow edema, and enhancement, and allowing the detection of intraspinal complications such as epidural abscess (Fig S6) (74). Absence of a soft-tissue mass can help differentiate discitis-osteomyelitis from Langerhans cell histiocytosis and neoplasms (eg, sarcoma, lymphoma, or neuroblastoma metastasis).

Conclusion

While there is considerable clinical and radiologic overlap, the gamut of acute pediatric head and neck diseases differs from that in adult patients. Knowledge of specific pediatric disease processes and normal developmental variants is critical for radiologists to provide timely and accurate diagnoses.

Author affiliations.—From the Department of Radiology, Monroe Carell Jr Children's Hospital at Vanderbilt, 2200 Children's Way, Nashville, TN 37232 (A.M.F., L.J., R.K., D.C.M., E.S., T.T., S.P., A.S.); Department of Radiology, Phoenix Children's Hospital, Phoenix, AZ (J.V.); and Department of Radiology, Children's Hospital of Philadelphia, Philadelphia, PA (K.S.). Presented as an education exhibit at the 2023 RSNA Annual Meeting. Received January 29, 2024; revision requested March 6 and received March 25; accepted April 23. **Address correspondence to** A.M.F. (email: *Alexandra.foust16@gmail.com*).

Disclosures of conflicts of interest.—**A.S.** Royalties or licenses from Cambridge University Press. **S.P.** Member of Sectra Advisory Board. All other authors, the editor, and the reviewers have disclosed no relevant relationships.

References

1. Yoong SYC, Ang PH, Chong SL, et al. Common diagnoses among pediatric attendances at emergency departments. BMC Pediatr 2021;21(1):172.
2. Radhakrishnan L, Carey K, Hartnett KP, et al. Pediatric Emergency Department Visits Before and During the COVID-19 Pandemic: United States, January 2019-January 2022. MMWR Morb Mortal Wkly Rep 2022;71(8):313–318.
3. Kutanzi KR, Lumen A, Koturbash I, Miousse IR. Pediatric Exposures to Ionizing Radiation: Carcinogenic Considerations. Int J Environ Res Public Health 2016;13(11):1057.
4. Artunduaga M, Liu CA, Morin CE, et al. Safety challenges related to the use of sedation and general anesthesia in pediatric patients undergoing magnetic resonance imaging examinations. Pediatr Radiol 2021;51(5):724–735.
5. Tipnis SV, Rieter WJ, Patel D, Stalcup ST, Matheus MG, Spampinato MV. Radiation Dose and Image Quality in Pediatric Neck CT. AJNR Am J Neuroradiol 2019;40(6):1067–1073.
6. Nagaraj UD, Koch BL. Imaging of orbital infectious and inflammatory disease in children. Pediatr Radiol 2021;51(7):1149–1161.
7. Ludwig BJ, Foster BR, Saito N, Nadgir RN, Castro-Aragon I, Sakai O. Diagnostic imaging in nontraumatic pediatric head and neck emergencies. RadioGraphics 2010;30(3):781–799.
8. Torretta S, Guastella C, Marchisio P, et al. Sinonasal-related Orbital Infections in Children: A Clinical and Therapeutic Overview. J Clin Med 2019;8(1):101.

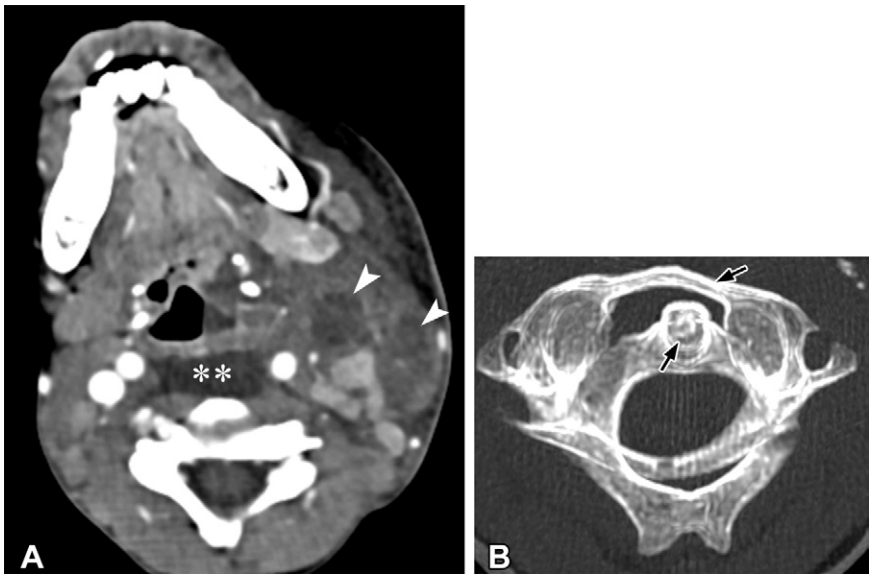

Figure 26. Grisel syndrome diagnosed in a 7-year-old boy with neck swelling and restricted movement. **(A)** Axial CECT image of the neck reveals suppurative lymphadenitis (arrowheads) and a large retropharyngeal effusion (*). **(B)** Axial maximum intensity projection bone CT image shows abnormal rotation and subluxation of C1 on C2 (arrows), which were repaired.

9. Reinshagen KL, Massoud TF, Cunnane MB. Anatomy of the Orbit. Neuroimaging Clin N Am 2022;32(4):699–711.
10. Foust AM, Estroff JA, Robson CD. Developmental Anomalies of the Midface. Neurographics 2023;13(2):46–63.
11. Ali MJ. Pediatric Acute Dacryocystitis. Ophthal Plast Reconstr Surg 2015;31(5):341–347.
12. Burns NS, Iyer RS, Robinson AJ, Chapman T. Diagnostic imaging of fetal and pediatric orbital abnormalities. AJR Am J Roentgenol 2013;201(6):W797–W808.
13. Maier C, Thieme N, Beck-Broichsitter B, et al. Imaging the Tight Orbit: Radiologic Manifestations of Orbital Compartment Syndrome. AJNR Am J Neuroradiol 2023;44(5):589–594.
14. Chung EM, Smirniotopoulos JG, Specht CS, Schroeder JW, Cube R. From the archives of the AFIP: Pediatric orbit tumors and tumorlike lesions—nonosseous lesions of the extraocular orbit. RadioGraphics 2007;27(6):1777–1799.
15. Passi N, Degnan AJ, Levy LM. MR imaging of papilledema and visual pathways: effects of increased intracranial pressure and pathophysiologic mechanisms. AJNR Am J Neuroradiol 2013;34(5):919–924.
16. Chang MY, Binenbaum G, Heidary G, et al. Imaging Methods for Differentiating Pediatric Papilledema from Pseudopapilledema: A Report by the American Academy of Ophthalmology. Ophthalmology 2020;127(10):1416–1423.
17. Chang MY, Pineles SL. Pediatric Optic Neuritis. Semin Pediatr Neurol 2017;24(2):122–128.
18. Ramanathan S, Prelog K, Barnes EH, et al. Radiological differentiation of optic neuritis with myelin oligodendrocyte glycoprotein antibodies, aquaporin-4 antibodies, and multiple sclerosis. Mult Scler 2016;22(4):470–482.
19. Nocon CC, Baroody FM. Acute rhinosinusitis in children. Curr Allergy Asthma Rep 2014;14(6):443.
20. Eloy P, Poirrier AL, De Dorlodot C, Van Zele T, Watelet JB, Bertrand B. Actual concepts in rhinosinusitis: a review of clinical presentations, inflammatory pathways, cytokine profiles, remodeling, and management. Curr Allergy Asthma Rep 2011;11(2):146–162.
21. Tekes A, Palasis S, Durand DJ, et al; Expert Panel on Pediatric Imaging. ACR Appropriateness Criteria Sinusitis: Child. J Am Coll Radiol 2018;15(11S):S403–S412.
22. Mafee MF, Tran BH, Chapa AR. Imaging of rhinosinusitis and its complications: plain film, CT, and MRI. Clin Rev Allergy Immunol 2006;30(3):165–186.
23. Koltsidopoulos P, Papageorgiou E, Skoulakis C. Pott's puffy tumor in children: a review of the literature. Laryngoscope 2020;130(1):225–231.
24. Sharma P, Sharma S, Gupta N, Kochar P, Kumar Y. Pott puffy tumor. Proc Bayl Univ Med Cent 2017;30(2):179–181.
25. Gupta AK, Bansal S. Rijuneeta, Gupta B. Invasive fungal sinusitis. Clinical Rhinology 2012;5(2):63–71.
26. Orman G, Kralik SF, Desai N, et al. Imaging of Paranasal Sinus Infections in Children: A Review. J Neuroimaging 2020;30(5):572–586.
27. Middlebrooks EH, Frost CJ, De Jesus RO, Massini TC, Schmalfuss IM, Mancuso AA. Acute Invasive Fungal Rhinosinusitis: A Comprehensive Update of CT Findings and Design of an Effective Diagnostic Imaging Model. AJNR Am J Neuroradiol 2015;36(8):1529–1535.
28. Kirsch CFE, Bykowski J, Aulino JM, et al; Expert Panel on Neurologic Imaging. ACR Appropriateness Criteria Sinonasal Disease. J Am Coll Radiol 2017;14(11S):S550–S559.
29. Mossa-Basha M, Ilica AT, Maluf F, Karakoç Ö, Izbudak I, Aygün N. The many faces of fungal disease of the paranasal sinuses: CT and MRI findings. Diagn Interv Radiol 2013;19(3):195–200.
30. Dixit R, Gupta A, Prakash A, Pradhan GS. Magnetic resonance imaging of rhino-orbito-cerebral mucormycosis: a pictorial review. Acta Radiol 2023;64(4):1641–1649.
31. Yi Z, Fang Z, Lin G, et al. Nasopharyngeal angiofibroma: a concise classification system and appropriate treatment options. Am J Otolaryngol 2013;34(2):133–141.
32. Rodriguez DP, Orscheln ES, Koch BL. Masses of the nose, nasal cavity, and nasopharynx in children. RadioGraphics 2017;37(6):1704–1730.
33. Baba A, Kurokawa R, Kurokawa M, Srinivasan A. MRI features of sinonasal tract angiofibroma/juvenile nasopharyngeal angiofibroma: case series and systematic review. J Neuroimaging 2023;33(5):675–687.
34. Ellika SK, Chadha M, Yang Z. Imaging in nontraumatic pediatric head and neck emergencies. J Pediatr Neurol 2017;15(5):263–293.
35. Lee JJW, Philteos J, Levin M, Namavarian A, Propst EJ, Wolter NE. Clinical Prediction Models for Suspected Pediatric Foreign Body Aspiration: A Systematic Review and Meta-analysis. JAMA Otolaryngol Head Neck Surg 2021;147(9):787–796.
36. Pugmire BS, Lim R, Avery LL. Review of Ingested and Aspirated Foreign Bodies in Children and Their Clinical Significance for Radiologists. RadioGraphics 2015;35(5):1528–1538.
37. Grey NEO, Malone LJ, Miller AL, et al. Magnetic resonance imaging findings following button battery ingestion. Pediatr Radiol 2021;51(10):1856–1866.
38. Riedesel EL, Richer EJ, Sinclair EM, et al. Serial MRI Findings After Endoscopic Removal of Button Battery From the Esophagus. AJR Am J Roentgenol 2020;215(5):1238–1246.
39. Clarke R. Pediatric Odontogenic and Paranasal Sinus Infections. Neuroimaging Clin N Am 2023;33(4):673–684.
40. Kamalian S, Avery L, Lev MH, Schaefer PW, Curtin HD, Kamalian S. Nontraumatic head and neck emergencies. RadioGraphics 2019;39(6):1808–1823.
41. Pattanaik D, Lieberman JA. Pediatric Angioedema. Curr Allergy Asthma Rep 2017;17(9):60.

42. Ishigami K, Averill SL, Pollard JH, McDonald JM, Sato Y. Radiologic manifestations of angioedema. Insights Imaging 2014;5(3):365–374.
43. Bochner RE, Gangar M, Belamarich PF. A Clinical Approach to Tonsillitis, Tonsillar Hypertrophy, and Peritonsillar and Retropharyngeal Abscesses. Pediatr Rev 2017;38(2):81–92.
44. Heikkinen J, Nurminen J, Velhonoja J, et al. MRI Findings in Acute Tonsillar Infections. AJNR Am J Neuroradiol 2022;43(2):286–291.
45. Ali SA, Kovatch KJ, Smith J, et al. Predictors of intratonsillar versus peritonsillar abscess: a case-control series. Laryngoscope 2019;129(6):1354–1359.
46. Hagelberg J, Pape B, Heikkinen J, Nurminen J, Mattila K, Hirvonen J. Diagnostic accuracy of contrast-enhanced CT for neck abscesses: a systematic review and meta-analysis of positive predictive value. PLoS One 2022;17(10):e0276544.
47. Sobol SE, Zapata S. Epiglottitis and croup. Otolaryngol Clin North Am 2008;41(3):551–566, ix.
48. Stroud RH, Friedman NR. An update on inflammatory disorders of the pediatric airway: epiglottitis, croup, and tracheitis. Am J Otolaryngol 2001;22(4):268–275.
49. Francis CL, Larsen CG. Pediatric sialadenitis. Otolaryngol Clin North Am 2014;47(5):763–778.
50. Robson CD, Juliano A. Head and Neck Imaging. In: Walters MM, Robertson RL, eds. Pediatric Radiology: The Requisites. 4th ed. New York, NY: Elsevier, 2015; 353–404.
51. Gosche JR, Vick L. Acute, subacute, and chronic cervical lymphadenitis in children. Semin Pediatr Surg 2006;15(2):99–106.
52. Hoang JK, Branstetter BF 4th, Eastwood JD, Glastonbury CM. Multiplanar CT and MRI of collections in the retropharyngeal space: is it an abscess? AJR Am J Roentgenol 2011;196(4):W426–W432.
53. Carroll W, Van Beck J, Roby B. Is vessel narrowing secondary to pediatric deep neck space infections of clinical significance? Int J Pediatr Otorhinolaryngol 2019;125:56–58.
54. Robson CD, Hazra R, Barnes PD, Robertson RL, Jones D, Husson RN. Nontuberculous mycobacterial infection of the head and neck in immunocompetent children: CT and MR findings. AJNR Am J Neuroradiol 1999;20(10):1829–1835.
55. Gaddikeri S, Vattoth S, Gaddikeri RS, et al. Congenital cystic neck masses: embryology and imaging appearances, with clinicopathological correlation. Curr Probl Diagn Radiol 2014;43(2):55–67.
56. Adams A, Mankad K, Offiah C, Childs L. Branchial cleft anomalies: a pictorial review of embryological development and spectrum of imaging findings. Insights Imaging 2016;7(1):69–76.
57. Steinklein JM, Shatzkes DR. Imaging of Vascular Lesions of the Head and Neck. Otolaryngol Clin North Am 2018;51(1):55–76.
58. Stence NV, Fenton LZ, Goldenberg NA, Armstrong-Wells J, Bernard TJ. Craniocervical arterial dissection in children: diagnosis and treatment. Curr Treat Options Neurol 2011;13(6):636–648.
59. Nash M, Rafay MF. Craniocervical Arterial Dissection in Children: Pathophysiology and Management. Pediatr Neurol 2019;95:9–18.
60. Little SB, Sarma A, Bajaj M, et al. Imaging of Vertebral Artery Dissection in Children: An Underrecognized Condition with High Risk of Recurrent Stroke. RadioGraphics 2023;43(12):e230107.
61. Aeschlimann FA, Twilt M, Yeung RSM. Childhood-onset Takayasu Arteritis. Eur J Rheumatol 2020;7(1 suppl):S58–S66.
62. Lui DH, Patel S, Khurram R, Joffe M, Constantinou J, Baker D. Mycotic internal carotid artery pseudoaneurysm secondary to *Mycobacterium tuberculosis*. J Vasc Surg Cases Innov Tech 2022;8(2):251–255.
63. Hudgins PA, Dorey JH, Jacobs IN. Internal carotid artery narrowing in children with retropharyngeal lymphadenitis and abscess. AJNR Am J Neuroradiol 1998;19(10):1841–1843.
64. Marom T, Roth Y, Boaz M, et al. Acute Mastoiditis in Children: Necessity and Timing of Imaging. Pediatr Infect Dis J 2016;35(1):30–34.
65. Vazquez E, Castellote A, Piqueras J, et al. Imaging of complications of acute mastoiditis in children. RadioGraphics 2003;23(2):359–372.
66. Campion T, Taranath A, Pinelli L, et al. Imaging of temporal bone inflammations in children: a pictorial review. Neuroradiology 2019;61(9):959–970.
67. Gadre AK, Chole RA. The changing face of petrous apicitis: a 40-year experience. Laryngoscope 2018;128(1):195–201.
68. Khan MA, Quadri SAQ, Kazmi AS, et al. A Comprehensive Review of Skull Base Osteomyelitis: Diagnostic and Therapeutic Challenges Among Various Presentations. Asian J Neurosurg 2018;13(4):959–970.
69. Trück J, Thompson A, Dwivedi R, Segal S, Anand G, Kelly DF. Nonotogenic Skull Base Osteomyelitis in Children: Two Cases and a Review of the Literature. Pediatr Infect Dis J 2015;34(9):1025–1027.
70. Álvarez Jáñez F, Barriga LQ, Iñigo TR, Roldán Lora F. Diagnosis of Skull Base Osteomyelitis. RadioGraphics 2021;41(1):156–174.
71. Lowry KC, Estroff JA, Rahbar R. The presentation and management of fibromatosis colli. Ear Nose Throat J 2010;89(9):E4–E8.
72. Spinnato P, Zarantonello P, Guerri S, et al. Atlantoaxial rotatory subluxation/fixation and Grisel's syndrome in children: clinical and radiological prognostic factors. Eur J Pediatr 2021;180(2):441–447.
73. Saleh ES, Vasileff CC, Omari AM, Khalil JG. The Diagnosis and Management of Pediatric Spine Infections. Cureus 2021;13(7):e16748.
74. Al Yazidi LS, Hameed H, Kesson A, Isaacs D. Spondylodiscitis in children. J Paediatr Child Health 2022;58(10):1731–1735.